NUCLEAR REORGANIZATION AND DYNAMICS DURING CANINE PARVOVIRUS INFECTION

Master`s thesis

University of Jyväskylä

Faculty of Mathematics and Science

Molecular Biology

Summer 2007

Hanna Smolander

PREFACE

The following research was conducted at the Department of Biological and Environmental Science at the University of Jyväskylä. First, I would like to thank the professor Maija Vihinen-Ranta for the opportunity to conduct my *pro gradu* work in her group. Thank you for providing me a chance to accomplish my dream to work with viruses.

The most special thanks belong to my supervisor Teemu Ihalainen. Thank you for taking the time to teach me all facts and techniques I needed to know. Thank you for sharing your excellent knowledge in confocal microscopy and image analysis. Thank you for encouraging me to ask questions. And thank you for answering them. Thank you for proofreading and critiquing the rough draft of my writing. Without your constant guidance this work would not have been as pleasent as it was.

I also wish to thank other members of the Maija-Vihinen Ranta group for helping me. Thanks to Einari Niskanen, Johanna Rinne, Mirka Salminen, Juulia Jylhävä and Jenni Reimari.

Last, but not least, I would like to thank my family, my friends and my boyfriend. I greatly thank you all for listening to my complaints, worries and frustrations and more importantly for believing in me.

Jyväskylän yliopisto
Matemaattis-luonnontieteellinen tiedekunta

Pro gradu – tutkielman tiivistelmä

Tekijä: Hanna Smolander
Tutkielman nimi: Tuman uudelleen järjestäytyminen ja dynamiikka koiran parvovirus infektiossa
English title: Nuclear reorganization and dynamics during canine parvovirus infection
Päivämäärä: 29.8.2007 **Sivumäärä:** 61
Laitos: Bio- ja ympäristötieteiden laitos
Oppiaine: Molekyylibiologia
Tutkielman ohjaaja(t): FT Maija Vihinen-Ranta, FM Teemu Ihalainen

---

Tiivistelmä:

Koiran parvovirus (CPV) löydettiin 1970-luvun lopulla. Sen tiedetään aiheuttavan aikuisille koirille vakavaa ripulia ja sydänlihastulehdusta pennuille. CPV-partikkeli muodostuu DNA-genomista, ja sitä suojaavasta ikosahedrisesta proteiinikuoresta (kapsidista). Genomi sisältää kaksi avointalukuraamia, joista ensimmäinen koodaa ei-rakenteellisia proteiineja 1 ja 2 (NS1 ja NS2) ja toinen rakenteellisia proteiineja 1 ja 2 (VP1 ja VP2). Parvovirusten NS1 proteiinin on havaittu toimivan viruksen elinkierron useissa eri tehtävissä.

Koiran parvovirus pystyy infektoimaan ainoastaan jakautumisvaiheessa olevia soluja. Infektio alkaa viruksen kiinnittyessä solun pinnalla oleviin transferriinireseptoreihin. Isäntäsoluun tunkeutuminen jatkuu klatriinivälitteisellä endosytoosireitillä, jota pitkin virus kulkeutuu kohti tumaa käyttäen apuna solun dynamiinivälitteistä kuljetuskoneistoa. Lopulta virus vapautuu endosytoosireitiltä solulimaan, ja tunkeutuu tumahuokosten kautta tumaan.

Tuma on hyvin pitkälle organisoitunut aitotumallisen solun keskus. Se sisältää kromosomaalisen aineksen lisäksi muita rakenteita, kuten PML- rakenteita, speckle-rakenteita, tumajyväsen ja cajal bodies- rakenteita.

Tutkimuksen tarkoituksena oli saada lisätietoa koiran parvovirus infektion tumansisäisistä tapahtumista. Kokeellisessa työssä tarkkailtiin koiran parvoviruksen NS1-proteiinin kolokalisaatiota eri tumarakenteiden (PML- ja speckle-rakenteiden) ja tumarakenteista löytyvien proteiinien (SUMO-1,2, PABP2 ja TFIIB) kanssa infektion eri aikapisteissä (8h, 12h, 16h, ja 24h). Tämän lisäksi tutkimme tuman koon ja interkromosomaalisen tilan muutosta CPV infektion aikana. Tutkimus suoritettiin pääasiassa konfokaalimikroskopialla, fluorensoivia konstrukteja kuvaten, ja kuvien sisältämän tiedon kvantitatiivisella analysoinnilla. Tutkimuksessa tarkkailimme myös TFIIB:n sitoutumista ja dynamiikkaa elävissä soluissa FRAP–kokeiden avulla.

Tutkimuksessa selvisi, että NS1 proteiini kolokalisoi etenkin PML:n ja TFIIB:n kanssa, mahdollisesti myös SUMO-1:n kanssa. SUMO-2:n ja PABP2:n välinen kolokalisaatio NS1:n kanssa sen sijaan osoittautui heikoksi. PABP2:n ja NS1:n keskinäinen sijainti toisiinsa nähden vaikutti kuitenkin mielenkiintoiselta, sillä proteiinit sijaitsivat usein hyvin lähellä toisiaan. Tulosten perusteella koiran parvovirus näyttäisi tarvitsevan isäntäsolun tuman proteiineja/rakenteita infektion aikana.

Elävillä soluilla suoritettujen kokeiden tulokset osoitti, että TFIIB oli tumajyväsessä ennen infektion alkua. Sen sijaan infektoiduissa ja fiksatuissa soluissa suurin osa TFIIB:stä sijaitsi tumaplasmassa. FRAP-kokeiden tulokset antoivat viitettä siitä, että TFIIB:n sitoutumisominaisuudet poikkeaisivat toisistaan ei-infektiivisissä ja infektiivisissä soluissa.

Tuman koon muutosta koskevat kokeet osoittivat tuman kasvavan infektion edetessä (0h-48h). Tämä tuman näennäinen suureneminen saattaa kuitenkin olla seurausta virus materiaalin suuresta tuotosta. Lisäksi on mahdollista, että vain suuremmat tumat selviävät infektion myöhäiseen vaiheeseen asti.

Avainsanat: Koiran parvovirus; NS1; PML; SUMO-1,2; TFIIB; PABP2; tuma

University of Jyväskylä **Abstract of Master`s Thesis**
Faculty of Mathematics and Science

Author: Hanna Smolander
Title of thesis: Nuclear reorganization and dynamics during canine parvovirus infection
Finnish title: Tuman uudelleen järjestäytyminen ja dynamiikka koiran parvovirus infektiossa
Date: 29.8.2007 **Pages:** 61
Department: Department of Biological and Environmental Science
Chair: Molucular Biology
Supervisor(s): Maija Vihinen-Ranta Ph.D., Docent, Teemu Ihalainen, MSc

Abstract:

Canine parvovirus (CPV) was found at the end of the 1970s. It is a small autonomous virus with single stranded DNA genome. This virus is a pathogen for dogs causing severe enteritic and myocarditis. The genome is protected by icosahedral capsid. Within the genome there are two open reading frames one encodes the non-structural proteins 1 and 2 (NS1 and NS2) and the other encodes the structural proteins 1 and 2 (VP1 and VP2). The NS1 has shown to be a fundamental factor in many process of viral life cycle.

CPV can only infect dividing cells. The viral infection begins when the CPV binds to the transferrin receptors (TfR) on the surface of the cell. After binding to the TfR the virus is quickly taken up into the cell via dynamin-dependent clathrin-mediated endocytosis. Following the endocytosis, the receptor-virus-complex is transported to the endosomes/lysosomes from where the CPV-capsid is released. Finally the virus enters to the nucleus via nuclear pore complex.

Nucleus is a highly organized center of eukaryotic cell. Besides the region of chromosomes it contains distinct structures such as cajal bodies, promyelocytic leukaemia bodies, nucleolus and nuclear speckles.

The current study was designed to investigate more about CPV infection and its effects on the nucleus and nuclear organelles. The colocalization between NS1 of CPV and nuclear bodies (PML NBs and nuclear speckle) as well as colocalization between NS1 and different nuclear proteins (SUMO-1, SUMO-2, TFIIB and PABP2) was examined at different time points of infection (8h, 12h, 16h, and 24h). In addition, the changes in the nucleus size and in the interchromosomal volume during CPV infection were studied. The colocalization and nuclear size analysis were conducted on a confocal microscope. After confocal imaging the data was quantitatively analyzed. Besides the colocalization studies the TFIIB was imaged in living cells. The possible binding properties of TFIIB was studied by using the FRAP technique.

This colocalization study of NS1 with different nuclear proteins demonstrated that the NS1 protein has similar localization with PML, TFIIB and at least partly with SUMO-1 protein. Any significant colocalization between NS1 and SUMO-2 or PABP2 was not discovered. However the NS1 and PABP2 interestingly appeared to locate next to each other.

The live cell imaging revealed that TFIIB localized mostly inside the nucleolus in non-infected cells. On the contrary when the cells were infected or fixed the great amount of TFIIB appeared mostly around the nucleoplasm. The FRAP experiments demonstrated that the TFIIB had various binding states in non-infected and infected cells.

The results of the nuclear size study indicated that the size expands during the CPV infection (0h-48h). Multiplied viral material could be one possible explanation for this “growth phenomena”. Another possibility for the results might be the lack of small nucleuses in later state of infection.

Keywords: Canine parvovirus; NS1; PML; SUMO-1, 2; TFIIB; PABP2; nucleus.

TABLE OF CONTENTS

ABBREVIATIONS 7

1 INTRODUCTION 9

1.1 CANINE PARVOVIRUS 9

1.1.1 Genome organization and structure *9*

1.1.2 Cell entry *10*

1.1.3 Non-structural protein 1 ..... *13*

1.2 NUCLEUS 15

1.2.1 Nuclear organelles *15*

1.2.2 Promyelocytic leukaemia nuclear bodies *16*

1.2.3 Nucleolus *17*

1.2.4 Cajal bodies *17*

1.2.5 Gems "the gemini of coiled bodies" *18*

1.2.6 Nuclear speckles *18*

1.3 NUCLEAR FACTORS 19

1.3.1 Small ubiquitin related modifiers *19*

1.3.2 Transcription factor II B *21*

1.3.3 Poly(A) binding protein 2 ..... *22*

1.3.4 Histone 2B *23*

2 AIM OF THE STUDY 25

3 MATERIALS AND METHODS 26

3.1 CELLS AND VIRUSES 26

3.2 TRANSFECTIONS AND INFECTIONS 26

3.3 ANTIBODY TREATMENTS 27

3.4 CONFOCAL MICROSCOPY 28

3.4.1 Colocalization experiment *29*

3.4.2 Live confocal microscopy *29*

3.5 IMAGE PROCESSING 31

4 RESULTS 32

4.1 COLOCALIZATION OF NS1 WITH NUCLEAR COMPONENTS 32

4.1.1 Colocalization between NS1 and EYFP-PML ... *32*
4.1.2 Colocalization between NS1 and EYFP-SUMO-1 ... *34*
4.1.3 Colocalization between NS1 and EYFP-SUMO-2 ... *36*
4.1.4 Colocalization between NS1 and EGFP-PABP2 ... *38*
4.1.5 Colocalization between NS1 and EGFP -TFIIB ... *40*
4.2 LIVE CELL IMAGING ... 43
4.2.1 FRAP ... *43*
4.3 CHANGE OF NUCLEAR SIZE DURING INFECTION ... 45
5 DISCUSSION ... **48**
5.1 THE COLOCALIZATION STUDIES ... 48
5.1.1 The interaction between PML and NS1 ... *48*
5.1.2 The interaction between SUMO-1 and NS1 ... *49*
5.1.3 The interaction between SUMO-2 and NS1 ... *49*
5.1.4 The interaction between PABP2 and NS1 ... *50*
5.1.5 The interaction between TFIIB & NS1 ... *50*
LIVE CELL IMAGING AND FRAP ... 52
5.1.6 FRAP (Fluorescence recovery after bleaching) ... *52*
5.2 THE SIZE OF NUCLEUS DURING INFECTION ... 54
REFERENCES ... **56**

ABBREVIATIONS

ATP	adenosine triphosphate
ATPase	enzyme that catalyzes the hydrolysis of ATP to ADP
BPV	bovine parvovirus
BSA	bovine serum albumin
CBP	cAMP response element binding protein
CBs	cajal bodies
CLK/STY	protein kinase
CMV	cytomegalovirus
CPV	canine parvovirus
Daxx	death-associated protein 6
DFC	dense fibrillar component of nucleolus
DMEM	dulbecco's modified eagle medium
DNA	deoxyribonucleic acid
EGFP	enhanced green fluorescent protein
EYFP	enhanced yellow fluorescent protein
FCs	fibrillar centers of nucleolus
FLIP	fluorescence loss in photobleaching
FPV	feline panleukopenia virus
FRAP	fluorescence recovery after photobleaching
GC	granular component of nucleolus
HCMV	human cytomegalovirus
HFV	human foamy virus
HSV-1	herpes simplex virus type 1
H2B	core histone 2B
IGCs	intercromatin granule clusters
IFN	interferon
IE1	immediate-early 1 protein
LSCM	laser scanning confocal microscopy
MOI	multiplicity of infection
MVM	minute virus of mice
NA	numerical aperture
NLFK	nothern laboratory feline kidney cells
NLS	nuclear location signal
NPC	nuclear pore complex
NS1 and NS2	non-structural proteins 1 and 2
ORF	open reading frame
PABP2	poly(A) binding protein 2
PAP	poly(A) polymerase
PBS	phosphate buffered saline,
PFA	paraformaldehyde
PIC	pre-initation complex of transcription

PLA_2	phospholipase A_2
PML	promyelocytic leukaemia protein
PML NBs	promyelocytic leukaemia protein nuclear bodies
PP1	protein phosphatase 1
P38	CPV promoter of capsid genes
P4	CPV promoter of non-structural protein genes
p 53	tumor supressor protein
p 73α	tumor supressor protein
Ran GAP1	signal transducer
RNA	ribonucleic acid
mRNA	messenger ribonucleic acid
rRNA	ribosomal ribonucleic acid
SAE1/SAE2	SUMO-1 conjugating enzyme
SMA	spinal muscular atrophy
SMN	gene called survival of motor neurons
snRNPs	small nuclear ribonucleoproteins
SnoRNP	nucleolar ribonucleic acid -protein complexes
S phase	part of cell cycle in which DNA synthesis occur
Sp100	a nuclear autoimmune antigen
SR-proteins	serine/arginine-residue proteins
SUMO-1, 2 and 3	small ubiquitin-related modifier-1, 2 and 3
TATA-box	A and T rich septamer before startpoit of RNA pol II
TBP	TATA-box binding protein
TFIIB	transcription factor II B
TFIIX	polymerase II transcription factors
TfR	transferrin receptor
UBC9	SUMO-1 conjugating enzyme
USP7 (HAUSP)	ubiquitin-specific protease 7
VP1, VP2 and VP3	viral (structural) proteins 1, 2 and 3

1 INTRODUCTION

1.1 Canine parvovirus

The family of *parvoviridae* comprises of large variety of small viruses with natural host ranging from primates to insects. This family is divided into two subfamilies: the *Parvovirinae* and the *Densovirinae*. The *Parvovirinae* subfamily on the other hand consists of six genera; *Amdovirus*, *Bocavirus*, *Dependovirus*, *Erythrovirus*, *Parvovirus* and *unclassified Parvovirinae* (7th report of ICTV).

The canine parvovirus (CPV) belongs to a genus of parvovirus (7th report of ICTV). Earliest observation of CPV was made in late 1970s. The sudden appearance of the virus implicated that it originated from already existing virus, presumably from feline panleukopenia virus (FPV) (for review see Parrish, C.R., 1990). This theory of origin is also supported by the fact that the genes of CPV and the FPV have more than 95 % similarity (Reed, A.P. et al., 1988). The CPV was discovered to be a new pathogen for dogs causing severe enteritic and myocarditis.

1.1.1 Genome organization and structure

Canine parvovirus is a humble non-enveloped virus. It has linear single-stranded (ss) DNA genome (5,323 nucleotides) with terminal palidromic structures. The genome encodes two structural (VP1 and VP2) and two non-structural proteins (NS1 and NS2). The non-structural proteins are translated from the open reading frame of the 3´end while the other open reading frame in the 5´end encodes the structural proteins (Cotmore, S.F., and Tattersall, P., 1987, Parrish, C.R., 1991, Reed, A.P. et al., 1988). Only the negative strand is enclosed inside the capsid (Reed, A.P. et al., 1988).

The capsid structure of canine parvovirus has been determined by X-ray crystallography. The DNA genome of CPV is protected by a 26 nm diameter icosahedral capsid which is assembled from 60 subunits of VP1, VP2 and VP3 proteins (Fig. 1.1) (Tsao, J. et al., 1991, Xie, Q., and

Chapman, M.S., 1996). The VP1 and VP2 are formed through alternating splicing of the viral mRNA whereas VP3 is formed by proteolytic cleavaging of the VP2 N-terminal (Paradiso, P.R. et al., 1982, Reed, A.P. et al., 1988). This cleavage reaction uncovers some glysine-rich sequences which are suggested to be necessary for virus to contact with cellular membranes (Tullis, G.E. et al., 1992). The VP1 contains the entire sequence of VP2 and in addition an extra domain in N-terminal required for infection (Vihinen-Ranta, M. et al., 1997).

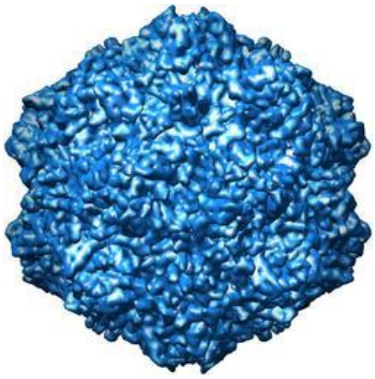

Figure 1.1. Capsid of canine parvovirus
(Virus particle database: http://viperdb.scripps.edu/redir.php)

The structural elements of the capsid are comprised of eight-stranded antiparallel β-barrel with large loops between strands (Tsao, J. et al., 1991). The cylindrical structure at fivefold axis of symmetry is composed of such β-barrel motifs. The connecting loops make up most of the outer surface. Moreover they form the “spike” like structures (22 Å long) at the threefold axes of symmetry and the cavity like depression at the twofold axes symmetry. In addition the connectiong loops form a canoyn-like depression (15 Å), surrounding the fivefold axis of symmetry (Tsao, J. et al., 1991, Xie, Q., and Chapman, M.S., 1996).

1.1.2 Cell entry

In order to start an infection, virus has to enter into the host cell. Viruses have different ways to penetrate into cells. The canine parvovirus uses receptor-mediated endocytosis for successful infection (Parker, J.S., and Parrish, C.R., 2000).

The ability of canine parvovirus to infect cells depends on the cell cycle. Autonomous parvoviruses can only infect cells which are in the process of dividing in other words at the S phase of the cell cycle. Initiation of a viral infection begins when the CPV attaches to the transferrin receptor (TfR) on the surface of the cell (Parker, J.S. et al., 2001). For that reason the TfR seems to be a critical factor of cell vulnerability to the virus infection. Primary function of the TfR is to deliver transferrin bound ferric iron inside the cell (Trowbridge, I.S., and Omary, M.B., 1981). The CPV has also been demonstrated to bind to sialic acid. Nonetheless, this binding does not mediate the infection (Barbis, D.P. et al., 1992).

After binding to the TfR the virus is quickly taken up into the cell via dynamin-dependent clathrin-mediated endocytosis (Parker, J.S., and Parrish, C.R., 2000). Following the endocytosis of clathrin-coated vesicles, the receptor-virus-complex is transported to the endosomes. Before the viral material can reach the nucleus it has to escape from the transporting vesicles (Parker, J.S. et al., 2001, Parker, J.S., and Parrish, C.R., 2000, Suikkanen, S. et al., 2002). The N-terminal of the VP1 protein has been illustrated to have a phospholipase A_2 like domain (PLA_2). The function of PLA_2 together with low pH-environment of late endosomal/lysosomal vesicles appears to help the virus to penetrate through the membrane of the vesicle. As a consequence the capsid is released to the cytoplasma into the perinuclear location (Suikkanen, S. et al., 2003b).

After the intact virus has released to the cytoplasma it is actively transported toward nucleus. The transfer occurs along microtubules with a help of dynein. The capsid is carried through the cytoplasma to the closeness of the nuclear pore. The nuclear location signal (NLS) in the N-terminal of VP1 (within capsid) directs the transport of the virus toward the nucleus. Finally the virus enters to the nucleus via nuclear pore complex (NPC). The CPV is sufficiently small virus to pass intact through the nuclear pore (Fig. 1.2) (Suikkanen, S. et al., 2003a, Vihinen-Ranta, M. et al., 2000).

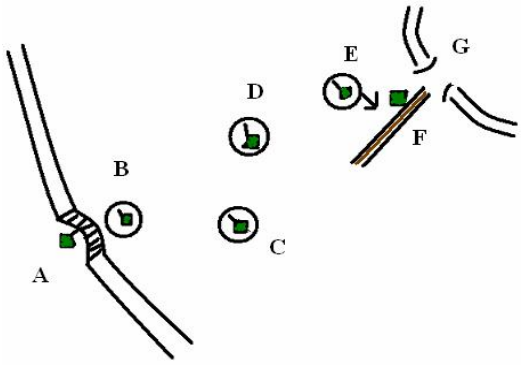

Figure 1.2. Life cycle of canine parvovirus. A: CPV attach to the TfR on the cell membrane, B: the clathrin coated vesicle is formed, C: early endosome, D: late endosome, E: lysosome, F: dynamin –dependent transport along microtubulus and G: nuclear pore (Drawn on based to the text).

The occurrence of NS1 protein of CPV is an evident sign of viral infection (Suikkanen, S. et al., 2002, Suikkanen, S. et al., 2003a). The NS1 protein has demonstrated to work as an initiator protein for viral DNA replication and as a transcriptional activator of the viral promoters.

1.1.3 Non-structural protein 1

The autonomous parvoviruses have largely same kind of genomic organization, for example canine parvovirus (CPV), feline panleukopenia virus (FPV) and minute virus of mice (MVM) have remarkably close relationship (Reed, A.P. et al., 1988). The genome of single stranded parvovirus is approximately 5,000 nucleotides in length and as previously mentioned it has two open reading frames (ORFs). The two non-structural proteins NS1 and NS2 are encoded from "early" P4 promoter (situated in 3´half) (Cotmore, S.F., and Tattersall, P., 1986, Pintel, D. et al., 1983).

The coding region of NS1 protein has been demonstrated to be extremely conserved between parvoviruses (except B19 human parvovirus). NS1 amino acids (352 to 516) of CPV have 90% or greater similarity to MVM (amino acids 399 to 564) (Reed, A.P. et al., 1988). The NS1 (83kDa) of MVM has been shown to be a fundamental factor in many process of viral life cycle. It is required for productive viral DNA replication, control of promoters and also for cytotoxic operation in the host cell (Nuesch, J.P. et al., 1998, Rhode, S.L., 3rd, and Richard, S.M., 1987).

The DNA replication of MVM is initiated by NS1 via site- and strand-specific nicking reaction. After introducing the strand-specific nick into origin sequences of replication, it joins covalently to the 5´end of the DNA at this site (Cotmore, S.F. et al., 1992, Cotmore, S.F. et al., 1993). The free 3´end hydroxyl generated by nicking reaction operates as a primer for DNA synthesis (Cotmore, S.F., and Tattersall, P., 1994). In addition the NS1 has ATPase and helicase activity, which are needed in replication (Wilson, G.M. et al., 1991).

The NS1 of MVM acts as a controller of promoters. The carboxy (C)-terminal domain of NS1 (acidic transcription activation domain) is able to function as an activator for P38 promoter, the promoter of capsid genes (Labieniec-Pintel, L., and Pintel, D., 1986). The NS1 enhances the P38 promoter activity and thus increases the expression of viral capsid proteins. On the other hand the large amount of NS1 has also been shown to inhibit the activity of P38 promoter (Corbau, R. et al., 1999, Legendre, D., and Rommelaere, J., 1994, Rhode, S.L., 3rd,

and Richard, S.M., 1987). The NS1 is considered to autoregulate its own P4 promoter to attain the most optimal concentrations for the activation of the P38 promoter (Rhode, S.L., 3rd, and Richard, S.M., 1987).

Furthermore NS1 can induce or repress other heterologous cellular and viral promoters (Corbau, R. et al., 1999, Legendre, D., and Rommelaere, J., 1994). The C- and amino (N)-terminal domains of NS1 most likely co-operate during regulatory functions. Because of the control activity has been demonstrated to localize in C-terminal the task of N-terminal is proposed to be recognition of the promoter. Both ends of NS1-protein are also functioning during cytotoxity activities (Fig. 1.3) (Legendre, D., and Rommelaere, J., 1992).

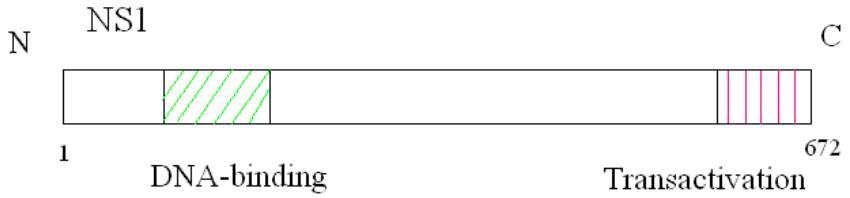

Figure 1.3. NS1 DNA binding site in N-terminal and C-terminal acidic activation domains (Modified from; http://www.sgm.ac.uk/jgvdirect/17649/17649ft.htm)

The NS1 activity of MVM is mainly regulated by posttranslation modification, by phosphorylation. At the beginning of infection NS1 become phosphorylated on serine and threonine residues. As the infection progresses the total expanse of phosphorylation increases. Different pattern of phosphorylation dominates different phase of infection (replication, transcription and cytotoxity) (Corbau, R. et al., 1999).

1.2 Nucleus

All eukaryotic cells have a nucleus. Quite recently the nucleus has been shown to be a highly organized center. Instead of being just a homogeneous gel-like structure, the nucleus has a number of compartmentalized domains and specialized organelles (Fig. 1.4) (for review see Matera, A.G., 1999, Lamond, A.I., and Sleeman, J.E., 2003).

1.2.1 Nuclear organelles

The nucleus is composed of different substructures which are not limited by a membrane but are still compartmentalized. Besides the region of chromosomes (euchromatin and heterochromatin regions) the nucleus contains distinct structures ("nuclear bodies") such as cajal bodies (CBs), promyelocytic leukaemia (PML) nuclear bodies (NBs), gems, nucleolus and nuclear speckles (Lamond, A.I., and Sleeman, J.E., 2003).

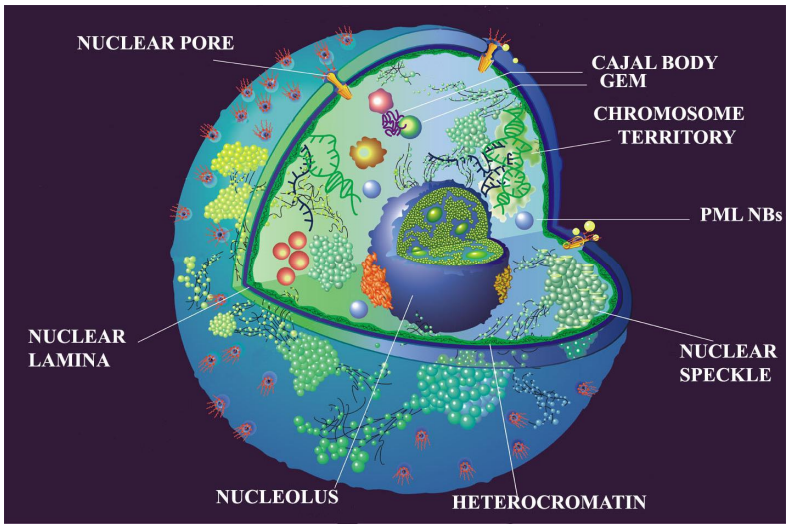

Figure 1.4. Structure of nucleus
(Modified from: http://spectorlab.cshl.edu/images/NucleusModel.jpg)

1.2.2 Promyelocytic leukaemia nuclear bodies

The promyelotic leukaemia (PML) protein belongs to a family of RING finger proteins with three cysteine-rich zinc-binding domains and a leucine coiled-coil domain (Freemont, P.S. et al., 1991). It is a major component of matrix connected PML nuclear bodies (NBs) (Zhong, S. et al., 2000a). The nucleus normally has 10-20 spherical PML NBs. The amount varies during cell-cycle and between different cell-types. The size is ranged between 0.3–1.0 μm in diameter (for review see Dellaire, G., and Bazett-Jones, D.P., 2004).

PML NBs are dynamic structures (Muratani, M. et al., 2002) containing several different proteins (besides PML-protein) such as Sp100 (nuclear antigen), SUMO-1 (Zhong, S. et al., 2000a), USP7 (HAUSP) (Everett, R.D. et al., 1997), CBP (transcriptional coactivator) (LaMorte, V.J. et al., 1998), Daxx (Zhong, S. et al., 2000b), p53 (tumor suppressors) (Zhang, Y., and Xiong, Y., 1999) and DNA helicase II. PML bodies have number of different functions such as regulation of transcription, protein storage, DNA repair, proteolysis, tumor suppression, apoptosis, sensors of cellular stress and interferon-induced antiviral defense (Dellaire, G., and Bazett-Jones, D.P., 2004).

PML NBs are suggested to have a certain role during viral infection. Especially DNA viruses have shown to interact with PML bodies. It has been demonstrated that for example viruses such as adenovirus, herpes simplex virus type 1 (HSV-1) (Everett, R.D., and Maul, G.G., 1994), cytomegalovirus (CMV) (Wilkinson, G.W. et al., 1998) and simian virus 40 (Ishov, A.M., and Maul, G.G., 1996) all have some kind of effect on PML bodies. Some of the viruses do not actually modify the PML NBs whereas others viruses have a drastic influence on PML bodies. For example the HSV-1 changes spherical PML NBs to filamentous and the CMV changes the localization and expression of PML NBs (Everett, R.D., and Maul, G.G., 1994, Ishov, A.M., and Maul, G.G., 1996).

Many states of viral infections can be prevented by interferon (IFN) mediate response. PML operates during IFN mediate antiviral defense by acting as an IFN induced cellular protein. For example in a case of the human foamy virus (HFV), the PML acts antivirally by

repressing transcription. The IFN activated PML (or the RING finger of PML) forms complex with transactivator, Tas, of HFV thus preventing it to work normally (Regad, T. et al., 2001).

1.2.3 Nucleolus

The nucleolus is a distinguishing dynamic nuclear sub-structure. It is not a permanent compartment. On the contrary it will associate and dissociate along the cell cycle. The nucleolus is a site where rRNA synthesis and assembly of ribosomal subunits (5.8S, 18S and 28S) is taken place. It can be divided into three sections; the fibrillar centers (FCs), the dense fibrillar component (DFC) and the granular component (GC). Different part of ribosomal assembly (from pre-rRNA to various ribosomal subunits) occurs in these separate sections (Lamond, A.I., and Sleeman, J.E., 2003).

1.2.4 Cajal bodies

Cajal bodies (CBs) discovered by Ramon y Cajal are remarkably conserved in evolution. CBs are dynamic structures which localize in the nucleolar periphery near gems (Dundr, M. et al., 2004, Liu, Q., and Dreyfuss, G., 1996). As well as many other nuclear organelles CBs are dependent of the cell cycle (Andrade, L.E. et al., 1993).

The CBs have been demonstrated to contain multiple nuclear factors including polymerase II transcription factors as well as factors meddling in pre-mRNA processing (see for review Matera, A.G., 1999). In addition the snRNPs and snoRNPs have assumed to maturate inside Cajal bodies (Sleeman, J.E., and Lamond, A.I., 1999).

Spinal muscular atrophy (SMA) is a deadly disease in which motor neurons are vanished from spinal cord leading paralysis and muscular deterioration. A gene responsible for SMA is called survival of motor neurons (*SMN*). Besides cytoplasma the SMN proteins are found to localize in and next to cajal bodies (see for review Frugier, T. et al., 2002).

1.2.5 Gems “the gemini of coiled bodies”

The existence of Gems was first found by studying the SMN protein. Gems highly resemble the cajal bodies (CBs). They appear to be very alike in number, size and localization. The spot like gems accommodate to cell cycle. They disappear during mitosis but will reappear in the nuclei of daughter cells. The role of gems is most likely closely related to function of CBs (Liu, Q., and Dreyfuss, G., 1996).

1.2.6 Nuclear speckles

Nuclear speckles or intercromatin granule clusters (IGCs) are small spot like subnuclear structures. 20-50 asymmetrical speckles (per nucleus) are located in the interchromatin space, scattered around the nucleoplasm. The speckles are very dynamic structures that break down during mitosis but will reassembly in nuclei of daughter cells (Spector, D.L. et al., 1991).

The nuclear speckles most likely operate as a “storehouse“or reassembly site for pre-mRNA splicing factors. This theory is supported by the fact that the size of nuclear speckles varies according transcription activity. When the transcription (as well as splicing) is prevented the size of speckles increases because the splicing factors clump together within speckles. Thus splicing factors move back and forth between active splicing sites and speckles (Spector, D.L., 1996).

The speckles contain hardly any DNA. In addition to the splicing factors needed in pre-messenger RNA processing (small nuclear ribonucleoproteins (snRNPs) and SR-proteins) (Spector, D.L., 1996) the speckles include multiple other factors; proteins for reversible phosphorylation (for example CLK/STY kinase and PP1 phosphatese) (Colwill, K. et al., 1996, Trinkle-Mulcahy, L. et al., 2001), mRNA 3´end processing factors (PAP and PABP2) and poly(A)$^+$ RNA population (Misteli, T., and Spector, D.L., 1997, Schul, W. et al., 1998, Spector, D.L., 1996). The reversible phosphorylation is considered to regulate the movements of speckle factors (Colwill, K. et al., 1996, Spector, D.L., 1996).

1.3 Nuclear factors

The above mentioned distinct nuclear organelles like PML NBs, nuclear speckles and cajal bodies are composed of multiple different nuclear factors. Consequently the large amount of certain factor is localized at specific and restricted regions inside the nucleus.

1.3.1 Small ubiquitin related modifiers

Mammals contain three different SUMO-encoding genes SUMO-1, SUMO-2 and SUMO-3. These post-translational modification proteins have implicated to have number of regulating functions. SUMO proteins regulate protein localization (Minty, A. et al., 2000), activity (Gostissa, M. et al., 1999), stability and mutual interaction by reaction called SUMOylation (Seeler, J.S. et al., 2001). The sumoylation happens mostly inside the nucleus and thus the target proteins of this modification reaction are nuclear proteins. The sumoylation reaction can be compared to ubiquitination. During both reactions the modifier is covalently attached to its target proteins.

The sumoylation is carried out by four sets of enzymatic reactions; maturation, activation, conjugation and ligation. First the C-terminal diglycine motif of SUMO is revealed by hydrolase (maturation reaction). Then the ATP-dependent activation event by E1 enzyme (SAE1/SAE2) occurs in which thioester bond between C-terminal glysine residue of SUMO and catalytic cysteine of E1 enzyme is formed (Desterro, J.M. et al., 1999, Okuma, T. et al., 1999). After that another thioesterbond is formed in conjugation reaction between E2 (UBC9) and SUMO (Schwarz, S.E. et al., 1998). Eventually the SUMO is attached to its target protein by an isopeptide bond (ligation reaction). ε-amino group of the lysine residue of the target protein is the attachment place for SUMO. This event is catalysed by UBC9 and E3 (ligase) together (Kotaja, N. et al., 2002, Schwarz, S.E. et al., 1998).

Three SUMO proteins that are expressed in mammalian cells differ from each other. The comparison of the amino acid sequences between SUMO-2 and SUMO-3 revealed 96% identity whereas SUMO-1 shares only ~ 46 % amino acid with abovementioned proteins

(Kamitani, T. et al., 1998). Besides the difference in homology, the function, dynamic of SUMO-2 and SUMO-3 are also shown to be dissimilar with SUMO-1. SUMO-2 and SUMO-3 are mostly found in free state while the SUMO-1 is found in more conjugated form (Ayaydin, F., and Dasso, M., 2004, Saitoh, H., and Hinchey, J., 2000).

The SUMO proteins have implicated to regulate multiple nuclear processes via sumoylation the target proteins such as; transcription factors (p53, p73α), signal transducers (Ran GAP1), viral proteins (BPV-E1), structural proteins (PML, sp100) and number of other proteins (Gostissa, M. et al., 1999, Matunis, M.J. et al., 1996, Minty, A. et al., 2000, Seeler, J.S. et al., 2001).

The SUMO-1 (Fig. 1.5) is also a critical factor during PML NBs formation. The published data establish that SUMO-1 modifies several PML NBs components and only when sumoylated these proteins are able to form PML NBs structures (Zhong, S. et al., 2000a).

Figure 1.5 3-D Structure of SUMO-1
(RCSB protein data bank; http://www.rcsb.org/pdb/home/home.do)

Many DNA viruses have demonstrated variously interfere with host cell's sumoylation "machinery". Viruses may prevent sumoylation of host proteins causing disorder, thus helping the viral conquest. For example the immediate-early 1 protein (IE1) of human cytomegalovirus (HCMV) desumoylates the PML NBs, as a consequence PML NBs becomes scattered (Everett, R.D., and Maul, G.G., 1994, Muller, S., and Dejean, A., 1999).

Viruses are also suggested to use the sumoylation "machinery" for their own purposes. They can use sumoylation to direct viral proteins to the correct location or to activate their transcriptional regulators. For example sumoylation of early protein (E1) of bovine

papillomavirus (BPV) controls success of the infection. Only correctly SUMO-modified E1 proteins manage to reach the right nuclear localization (Rangasamy, D. et al., 2000).

1.3.2 Transcription factor II B

Eukaryotic transcription begins from assembly of a preinitiation complex (PIC). This complex includes several different factors such as TFIID, TFIIB, TFIIA, TFIIF, TFIIE, TFIIH and RNA polymerase II. The above-mentioned factors attach to the complex in exact order. At first the TATA-binding subunit (TBP) of TFIID factor recognizes promoters and binds to the TATA-box. Next other transcription factors bind to this apparatus in following order; TFIIA, TFIIB, TFIIF, RNA polymerase II, TFIIE and TFIIH.

Together with TFIID the TFIIB has part of promoter recognition process, thus determinating the initiation site of transcription. Studies has shown that TFIIB binds both upstream and downstream of the TATA-box (Bushnell, D.A. et al., 2004). In addition, the TFIIB directs the RNA polymerase II to the right position of the initiation complex. The RNA polymerase II connects to the initiation complex via TFIIB (Malik, S. et al., 1993).

The structure of TFIIB (predicted MW 34.8 kDa) consist of three different portions; a zinc ribbon domain (in N-terminal, $TFIIB_N$), a finger domain and a C-terminal domain ($TFIIB_C$) (Fig. 1.6) (Bushnell, D.A. et al., 2004). Diverse domains are demonstrated to display different functional interactions (Barderis, A., et al 1993, Buratowski, S., and Zhou, H., 1993, Malik, S. et al., 1993). The flexible $TFIIB_{N,}$ the zinc finger domain, is responsible for interacting with RNA polymerase II. The finger domain is also shown to influence in the active center of polymerase II whereas the function of the tightly folded $TFIIB_C$ is to interact with TATA-binding protein (TBP) on DNA (Barberis, A., et al 1993). In addition the TFIIB stabilize formation of DNA-RNA hybrid. There is also a “region” called linker between the C-terminal and finger domain (Buratowski, S., and Zhou, H., 1993, Bushnell, D.A. et al., 2004)

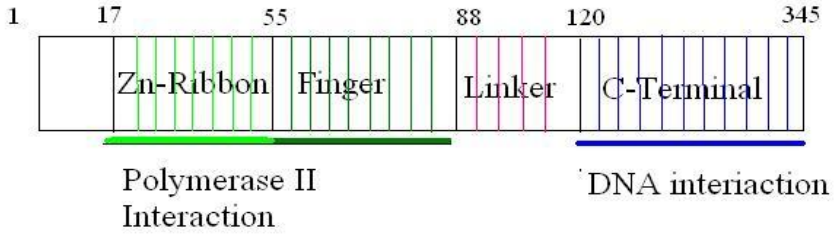

Figure 1.6 Domain structure of TFIIB (Modified from; Bushnell, D.A. et al., 2004)

Closer studies of the general transcription factor TFIIB have also revealed this factor acting as a target of acidic activators and steroid hormone reseptors (Ing, N.H. et al., 1992, Malik, S. et al., 1993).

1.3.3 Poly(A) binding protein 2

Most messenger RNAs of eukaryotic cells are post-translationally modified in nucleus before taking to the cytoplasm. The nuclear process of pre-mRNA includes; capping, splicing and polyadenylation. During the reaction of polyadenolation 200-250 adenosine residues are attached to the 3`end of mRNA.

Polyadenylation reaction contains two steps. First the pre-mRNA is cleaved at the specific site. The cleaving site is identified from conserved sequence (AAUAAA) which localizes 10-30 nucleotides upstream of the cutting and polyadenylation site. The GU or U sequence downstrean from cleaving site plays also part in recognition. After cleaving the polyadenylation is taken place (see for review Wahle, E., and Ruegsegger, U., 1999).

The poly(A) binding protein 2 (PABP2) is a critical factor in polyadenylation reaction (Fig. 1.7). It tightly attaches to the progressive poly(A) tails and promotes the addition of adenosine residues until the lenght of the tail is accomplished (approximately 250 residues). Besides the addition of adenosine residues PABP2 supervise that the size of poly(A) tail will be correct (Wahle, E. et al., 1993, Wahle, E., 1995).

Figure 1.7 PABP2 during polyadenylation reaction
(Modified from: www.steve.gb.com/science/transcription.html)

Studies have revealed that the PABP2 concentrates in irregular nuclear speckles (Krause, S. et al., 1994). Like TFIIB the PABP2 have bipartive structure. The N-terminal is composed of highly acidic amino acids (31 residues glutamate) whereas the C-terminal is very basic (arginines). Structually two different kinds of terminals have also varying functions. The N-end domain is resbonsible for binding the RNA and the C-end enable PABP2 to multimerize on poly(A) tails (Kuhn, U., and Pieler, T., 1996, Nemeth, A. et al., 1995).

1.3.4 Histone 2B

The eukaryotic chromatin forms “a neclace of pearls” like structure. The essential parts of the chromatin are nucleosomes which are composed of approximately 145-147 base pair (bp) of DNA wrapped around histone octamer (two copies of four different kinds of core histones H2A, H2B, H3 and H4).

Histone-2B (H2B) is regulated via post-translational modification for example acetylation, phosphorylation, deacetylation, methylation, sumoylation, ADP-ribosylation and ubiquitination (Davie, J.R., and Murphy, L.C., 1990, Golderer, G., and Grobner, P., 1991, Ito, T. et al., 2000, Nathan, D. et al., 2006, De la Barre, A.E. et al., 2001). In order to start the transcription, the chromatin needs to be remodeled by acetylation reaction. When acetylated, the H2A-H2B complex transfers from nucleosomes to histone chaperones (Ito, T. et al., 2000). The phosphorylation of histone N-terminal on the other hand is essential to chromatin condensation. Thus the above mentioned reaction is resbonsible of chromosome assembly (De la Barre, A.E. et al., 2001). The ubiquitination of the H2B is indicated to participate in gene activation (Davie, J.R., and Murphy, L.C., 1990). On the contrary to ubiquitination, the

sumoylation reaction of the H2B has demonstrated to affect negatively to the transcription level (Nathan, D. et al., 2006).

2 AIM OF THE STUDY

(I) To study the CPV infection after nuclear entry and to assess the viral effects of CPV on the nucleus and nuclear substructures.

(II) To determinate the possible interaction of non-structural protein 1 (NS1) with nuclear bodies and with nuclear proteins.

3 MATERIALS AND METHODS

3.1 Cells and viruses

Norden laboratory feline kidney cells (NLFK) were cultured and maintained in a mixture of Dulbecco's modified Eagle medium (DMEM, Gibco, Paisley, UK) supplemented with 10 % fetal bovine serum (BSA), antibiotics (penicillin and streptomycin) and non-essential amino acids. NLFK cells were maintained in 75 cm^2 flasks at 37 °C in a humified incubator with 5 % CO_2 and seeded twice a week. For studies the NLFK cells were grown on 11 mm diameter coverslips.

Canine parvovirus type 2 (CPV-d) was used in infections at MOI of 0.5-1 (a kindly gift from C.R. Parrish) (Parrish, C.R., 1991). Stock of viruses was stored at 4 °C.

3.2 Transfections and infections

For studies of NS1 colocalization with different nuclear components, NLFK cells were transfected with plasmids containing either EYFP-SUMO-1, EYFP-SUMO-2 (gifts from Dr. Mary Dasso) (Ayaydin, F., and Dasso, M., 2004), EYFP-PML (a gift from Dr. R. Everett) (Everett, R.D. et al., 2003), EGFP-PABP2 (a gift from Dr. Carmo-Fonseca) (Calapez, A. et al., 2002) or EGFP-TFIIB (a gift from Dr. S. Huang) (Chen, D. et al., 2002). The cells were also transfected with EYFP-H2B (a gift from Dr. Jörg Langowski) (Weidemann, T. et al., 2003) for analysis of nuclear size change during infection.

Transfections were done by Fugene or Mirus reagent as well as by electroporation (ECM 600 electroporator). When the cells were transfected with Fugene reagent, 1.5 µg of DNA and 6 µl of reagent were used. With Mirus reagent, 1 µg of DNA and 2-8 µl of reagent were utilized. The transfections were done according the manufacturer's instructions. For electroporation the settings were; mode (T): 500 V capacitance & resistance low voltage (LV), capacitance (C): 600 uF, resistance (R): R1 (13 ohm), champer gap: BTX disposable cuvette P/N 620 (2 mm gap), charging voltage (S): 130 V, estimated field strenght: 0.65 kV/ cm and targetted pulse

lenght: 7 ms.

For colocalization studies 80 % confluent, transfected cells grown on coverslips (in 3 cm Ø) were inoculated with CPV-2 multiplicity of infections 0.5-1 (1 µl of purified CPV-2 virus was diluted in 30 µl of DMEM and added to coverslip). After 20 min of incubation in 37 °C two more millilitres of DMEM was added. The positioning of NS1 protein of CPV and diverse fluorecent tagged components (EYFP-SUMO-1, EYFP-SUMO-2, EYFP-PML EGFP-PABP2 or EGFP-TFIIB) was studied with Olympus FluoView 1000 confocal microscope at different post infection (p.i.) time points (8h, 12h, 16h and 24h).

3.3 Antibody treatments

Prior to labeling the paraformaldehyde (PFA) fixed cells were treated with permeabilization buffer (containing 1 % bovine serum albumin (BSA), 1 % Triton X-100, and 0.01 % sodium azide in PBS) for 20 min to permeate the membranous elements in the cell. Then the coverslips were incubated with primary antibodies (a mouse monoclonal antibody (Mab) to nonstructural protein 1 (NS1)) for an hour at room temperature. Primary antibody was diluted into permeabilization buffer (concentration 1 µg/ml).

Before incubation with secondary antibody (Alexa-633-conjugated goat anti-mouse IgG) coverslips were washed twice with permeabilization buffer and once with PBS each wash lasting 20 min. The secondary antibody was incubated for 30 min at room temperature. Alexa-633-conjugated goat anti-mouse IgG was also diluted in permeabilization buffer (concentration 10 µg/ml).

After the secondary antibody treatment the coverslips were rinsed once with permeabilization buffer and twice with PBS each wash lasting 20 min and finally embedded with mowiol-DABCO and maintained at + 4 °C in dark.

3.4 Confocal microscopy

Laser scanning confocal microscopy (LSCM) is a powerful tool to observe a thin plane from thick specimen (Fig. 3.1). The microscope optically sections the specimen into different planes (x, y and z) which enables to achieve a three-dimensional (3D) data. These data can be presented as a projection.

The confocal microscopy is based on pinholes. The excitation light emitted by the laser system passes throught the first pinhole which targets the light beam via dichromatic mirror towards the specimen. An objective lens focuses the laser beam on the desired focal plane of the sample. The second pinhole located in front of the photodetector limits the observed light (fluorescence emission) coming from the sample. For that reason the detector perceive very little out-of-focus light (for review see Wright, S.J., and Wright, D.J., 2002). In this study the specimens containing multiple fluorescent probes were detected separately using different exitation wavelengths emissoin filters and sequential scanning to avoid false colocalization.

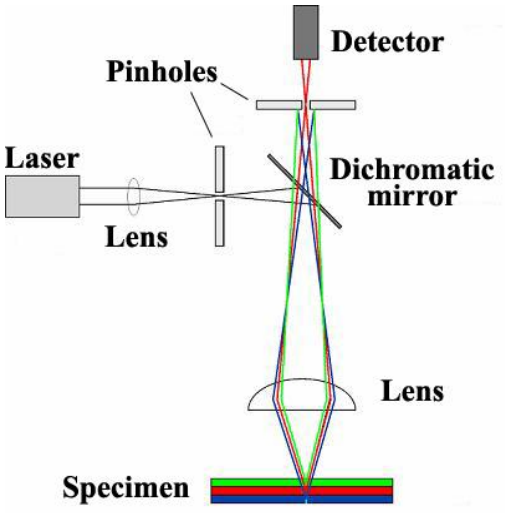

Figure 3.1 Principle of confocal microscopy
(Modified from: http://www.uni-mainz.de/FB/Chemie/AK-Janshoff/137_DEU_HTML.php)

Confocal microscopy of colocalization and nuclear size analysis were conducted on an Olympus FluoView 1000 confocal microscope using 60x APO oil immersion objective numerical aperture (NA) 1.4. Stacks of 20-30 images of 512 x 512 pixels (pixel resolution 92 nm/pixel) were collected using zoom factor 4.5. The fluorophores in the specimen were examined by using the excitation and emission appropriate for each dye. For EYFP and EGFP a 514 nm argon laser was used and the fluorescence was collected with a 525-565 nm band-pass filter. Whereas Alexa-633 was excited with a 633 nm helium-neon laser and the fluorescence was collected with a 650 nm long-pass filter.

3.4.1 Colocalization experiment

The idea of colocalization studies was to examine the positioning of NS1 protein with different nucler proteins; EYFP-SUMO-1, EYFP-SUMO-2, EGFP-TFIIB, EGFP-PABP2 or EYFP-PML. In confocal experiments both fixed and live cells were used and at least twenty cells per time point were examined. Colocalization percentages of NS1 and nuclear components (mentioned earlier) were calculated from the confocal images using ImageJ software and colocalization threshold plugin (Abramoff, 2004).

3.4.2 Live confocal microscopy

To study the dynamics of the EGFP-TFIIB the fluorescent labelled protein was visualized in living cells. By live cell imaging it was possible to avoid the possible false results caused by fixation.

In live cell studies, a Zeiss LSM 510 inverted laser scanning confocal microscope was used with 63x Plan-Neofluar oil immersion objective numerical aperture 1.25. The imaging settings used were; depth of data 8-bit, image size 256 x 256, pixel resolution 100 nm/pixel and maximum scan speed. The 488 nm argon laser was used for excitation and the fluorescense was collected with a 530-600 nm bandpass filter. The power of laser was 0.25 % during regular imaging and 100 % in bleaching. The tempcontrol property of Zeiss enabled to keep the temperature at 37 °C during the imaging.

Fluorescence recovery after photobleaching (FRAP) is a technique in which a high intensity laser is used to bleach out the fluorescence from accurately defined area. After the bleaching, fluorescence recovery is followed (Fig. 3.2). The recovery dynamics give information about protein diffusion, binding and other dynamic properties. To measure the rate and level of recovery of the fluorescent signal caused by EGFP-TFIIB, FRAP analysis was conducted to the EGFP-TFIIB expressing cells.

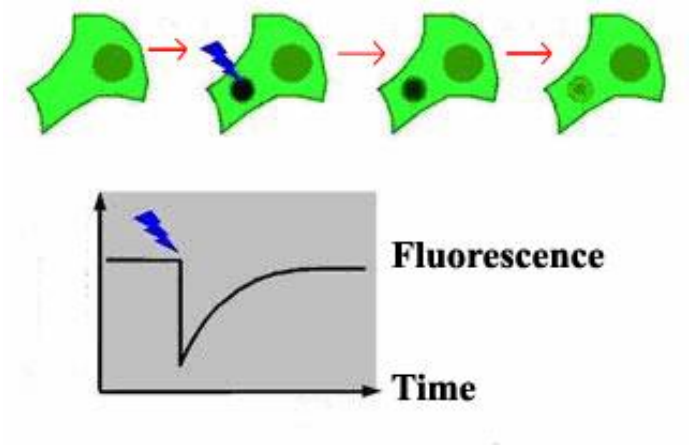

Figure 3.2 Principle of FRAP (fluorescence recovery after photobleaching)
(Modified from: http://www.answers.com/topic/fluorescence-recovery-after-photobleaching)

Before the FRAP was conducted the imaging conditions were optimised. The bleaching was minimized by observing the control cells and adjusting the laser power so low (0.25 %) that during the regular imaging there were hardly any loss of fluorescence signal. In addition, the loss of fluorescence in the whole cell due the bleach procedure (Fluorescence loss in photobleaching, FLIP) was measured in real time with bleach control experiments. The FRAP process was conducted on a circular area of 2 μm in diameter using a frame rate of 40 ms (25 frames per second). Finally, after the imaging, the data was normalized between 0 and 1. In normalization, the FLIP was taken account and the recovery was normalized to the fluorescence level before the bleach procedure.

3.5 Image processing

The images taken by Olympus FluoView 1000 confocal microscope were quantitatively processed by ImageJ software (Abramoff, 2004). For colocalization analysis the both image stacks (NS1 and the stack of either SUMO-1, SUMO-2, PML, TFIIB or PABP2) were opened and changed from 16-bit to 8-bit. Then the nucleus of interest was circled from both stacks and the outside cleared (command "clear outside") in order to get rid of extraneous objects near an item of interest. After that the background was subtracted (command "subtract background"). The colocalization analysis was made using plugin "colocalization threshold". Analyses measure the overlapping pixels between these two stacks. The TFIIB and PABP2 stacks were also smoothed and filtered before colocalization analysis. The aim was to get rid of the disruptive nucleoplasmic fluorescence. This was done because the TFIIB and the PABP2 were more homogenous inside the nucleus than SUMO-1, SUMO-2 or PML.

The purpose of H2B images was to find out if the volume of the nucleus or the interchromosomal space changed during the infection. This was achieved by calculating the volume of nucleus and the volume of chromatin. First the image stack of H2B was opened. The type was changed from 16-bit to 8-bit, outside was cleared and the stack was smoothed. Then the image stack was inverted in order to prevent the white being automatically selected as background. The function "threshold" was needed while creating binary images, after which images had only two intensity levels (0 or 255). To calculate the volume of chromatin the image stack was inverted back after which the command of particle analysis 3-D objects counter was used.

To calculate the volume of nucleus all the holes in the nuclear membrane were filled by choosing command "dilate". Then the area within the membrane was filled (command "fill holes"). Next the function of "erode" was used in order to return increased area of nucleus back to normal since the function of dilate increases the total area of nucleus. Finally the image was inverted back and the volume of nucleus was calculated by command particle analysis 3-D objects counter. The unoccupied interchromosomal space is the result of subtraction ("interchromosomal space=volume of nucleus – volume of chromatin").

4 RESULTS

4.1 Colocalization of NS1 with nuclear components

Study of the colocalization between the NS1 protein (primary anti-NS1, secondary Alexa-633) and one of the nuclear proteins; EYFP-PML (marker for PML NBs), EYFP-SUMO-1, EYFP-SUMO-2, EGFP-PABP2 (marker for nuclear speckles) or EGFP-TFIIB at different time of post infection (8h, 12h, 16h and 24h) was conducted with the Olympus FV-1000 confocal microscope. Twenty or more image stacks were taken from each time point.

After confocal imaging the data from the image stacks was analyzed with ImageJ software (Abramoff, 2004). With colocalization threshold plugin of ImageJ the colocalization percentages were counted from the merged images by companying the number of colocalized pixels to the total number of fluorescent pixels above the threshold. The threshold was automatically calculated according to Pearson`s correlation coefficient. The average colocalization of nuclear proteins with NS1 protein was calculated from the image stacks toward each time point.

4.1.1 Colocalization between NS1 and EYFP-PML

The confocal images taken from NS1 and PML fused to enhanced yellow fluorescent protein indicated that there were colocalization between these two proteins or at least they were positioned relatively close to each other at early phase of infection (8h-12h). While the infection proceeded (16h) the NS1 protein seemed to cover the whole nucleus and PML NBs. However, at 24h post infection the PML structures appeared to localize in places which included no NS1 protein (Fig. 4.1).

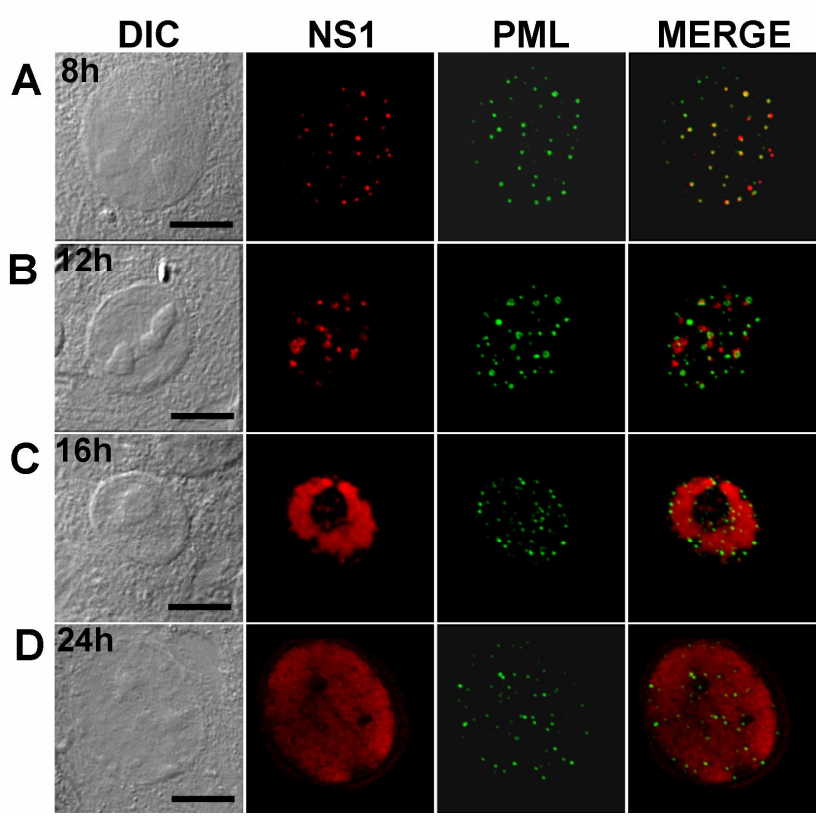

Figure 4.1 Panel of EYFP-PML and NS1 (DIC, NS1, EYFP-PML and merge) A) 8h p.i., B) 12h p. i., C) 16h p. i. and D) 24h p.i. In DIC pictures the scale bare is 5 μm.

Closer examination of the data from previous confocal images by ImageJ software showed quite high colocalization percents. The results indicated that the EYFP-PML colocalize significantly with NS1 protein at 8h time point. The amount of PML colocalizing with NS1 at 8h post infection was 33 ± 20 %, at 12h 19 ± 17 %, at 16h 47 ± 17 % and at 24h 41± 20 %. The variation of the data was similar during each time point (Fig. 4.2).

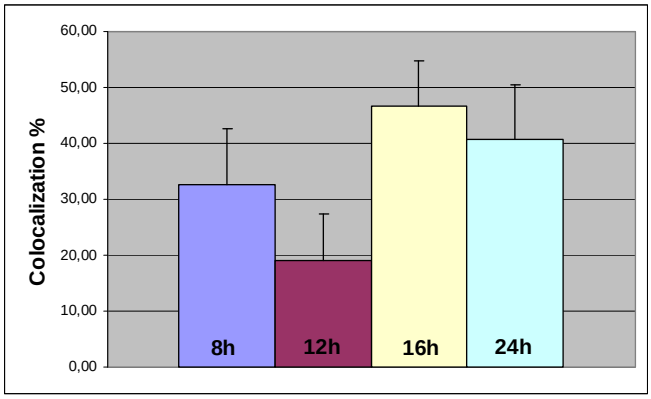

Figure 4.2 Histogram of the average colocalization percents between NS1 and EYFP-PML at four different time points (8h, 12h, 16h and 24h) and the variation of the data.

4.1.2 Colocalization between NS1 and EYFP-SUMO-1

Next we investigated whether enhanced yellow fluorescent protein fused to SUMO-1 colocalizes with NS1-foci. By examining only the confocal images the conclusion was made that at early phase of infection (8h-12h) the colocalization was not clearly detectable. At later time points of infection the NS1 filled the whole nucleus and covered the SUMO-1 positive structures (Fig. 4.3).

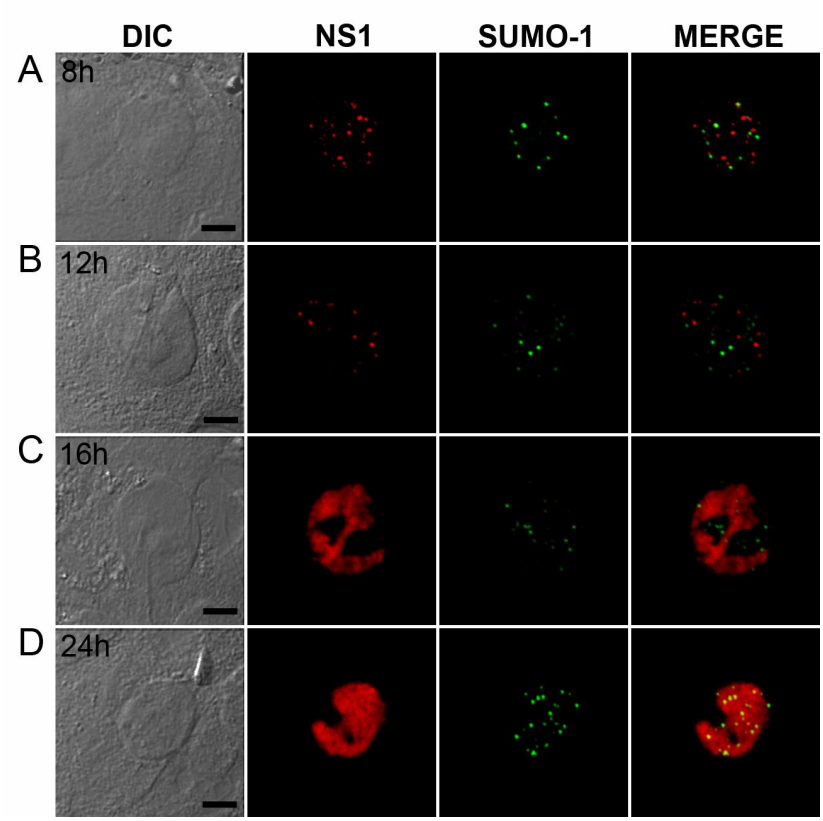

Figure 4.3 Panel of EYFP-SUMO-1 and NS1 (DIC, NS1, EYFP-SUMO-1 and merge) A) 8h p.i., B) 12h p.i., C) 16h p.i. and D) 24h p.i.. In DIC pictures the scale bare is 5 μm.

The data analysis of confocal images of NS1 and SUMO-1 showed similar pattern as the data earlier with NS1-foci and PML NBs (Fig. 4.1.). Colocalization percent was higher at 8h (20 ± 33 %) than at 12h (8 ± 13 %). During later time points of infections the degree of colocalization followed the amount of NS1. The amount of SUMO-1 colocalizing with NS1 was 21 ± 22 % at 16h and 48 ± 35 % at 24h (Fig. 4.4). Calculations were done by ImageJ.

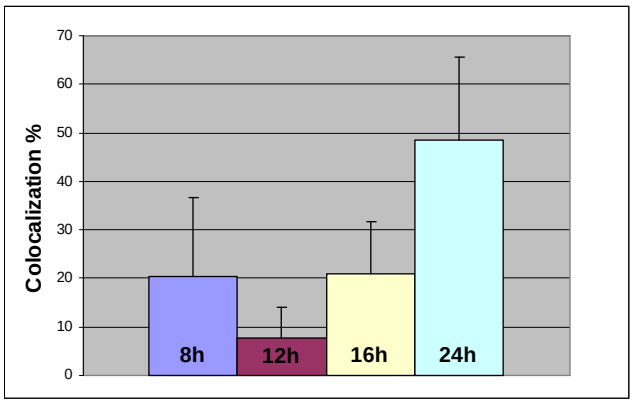

Figure 4.4 Histogram of the average colocalization percents between NS1 and EYFP-SUMO-1 at four different time points (8h, 12h, 16h and 24h) and the variation of the data.

4.1.3 Colocalization between NS1 and EYFP-SUMO-2

To identify the colocalization pattern of NS1 and enhanced yellow fluorescent protein linked to SUMO-2 same studies as previously were performed. From the confocal images it was quite easy to point out that the colocalization between these two proteins was rather insignificant. The colocalization could only be detected when infection had proceeded to the later phase (16h- 24h) (Fig. 4.5).

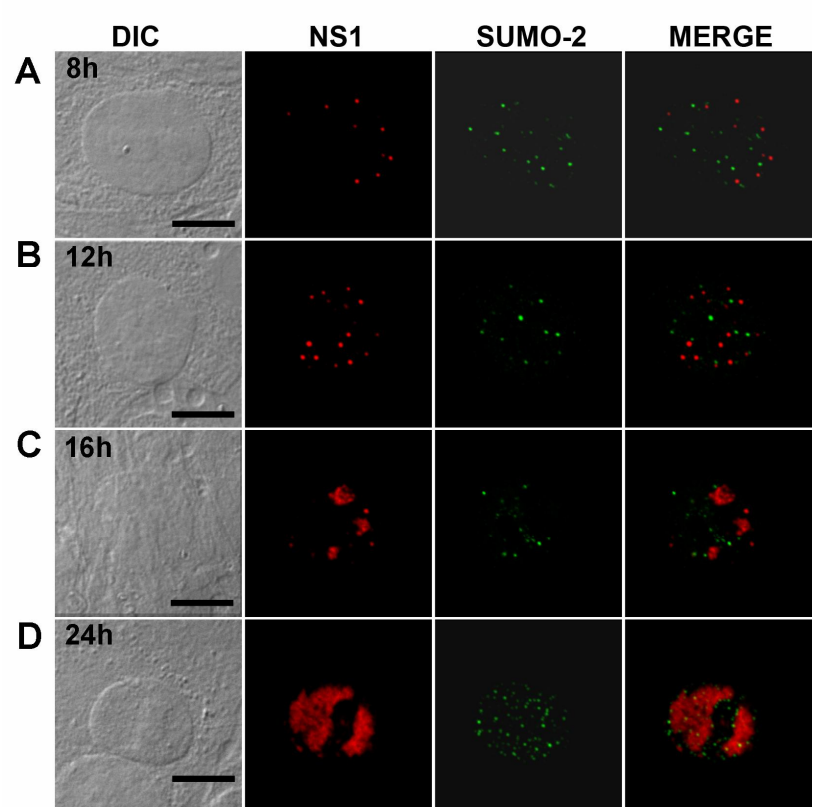

Figure 4.5 Panel of EYFP-SUMO-2 and NS1 (DIC, NS1, EYFP-SUMO-2 and merge) A) 8h p.i., B) 12h p.i., C) 16h p.i. and D) 24h p.i.. In DIC pictures the scale bare is 5 μm.

The quantitative analysis of the results by ImageJ suggested that the colocalization percents between NS1 and SUMO-2 increased proportionally to the infection. The colocalization grew as the infection progressed. The amount of SUMO-2 colocalizing with NS1 was; at 8h 1 ± 4 %, at 12h 6 ± 15 %, at 16h 14 ± 18 % and at 24h 42 ± 22 % (Fig. 4.6).

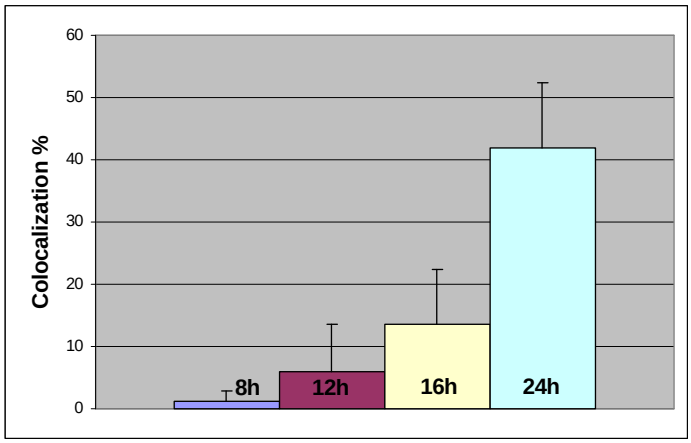

Figure 4.6 Histogram of the average colocalization percents between NS1 and EYFP-SUMO-2 at four different time points (8h, 12h, 16h and 24h) and the variation of the data.

4.1.4 Colocalization between NS1 and EGFP-PABP2

The confocal pictures from NS1 and enhanced green fluorescent protein linked to PABP2 turned out to be very interesting. By studying these pictures, the colocalization "pattern" looked dissimilar with above mentioned constructs. During the early phase of infection (8h-12h) the PABP2 and NS1 seemed to lie next to each other but on the contrary at 16h and 24h time points these two fluorescent proteins appeared to despise one another. During later phase of infection the PABP2 was located in spot like space where no NS1 was present (16h- 24h) (Fig. 4.7).

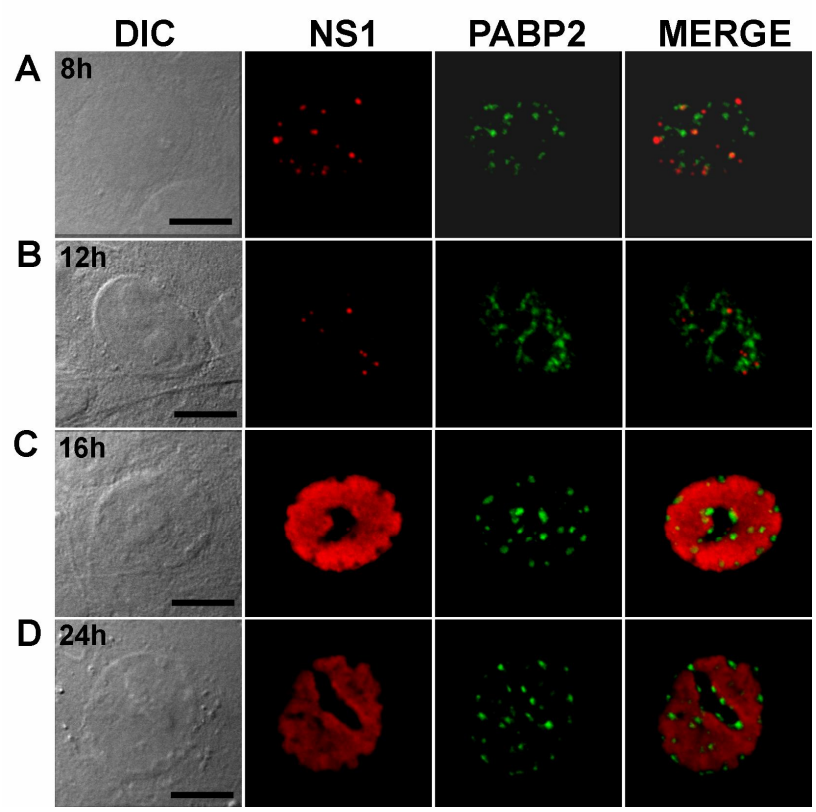

Figure 4.7 Panel of EGFP-PABP2 and NS1 (DIC, NS1, EGFP-PABP2 and merge A) 8h p.i., B) 12h p.i., C) 16h p.i. and D) 24h p.i.. In DIC pictures the scale bare is 5 µm.

Closer data analysis of NS1 and EGFP-PABP2 colocalization by ImageJ supported the presumption that was made according the confocal pictures. The average colocalization percents remained rather low even in later phase of infection. The amount of PABP2 colocalizing with NS1 was; at 8h 7 ± 9 % at 12h 8 ± 10 % at 16h 30 ± 21 % and at 24h 24 ± 18 % (Fig. 4.8).

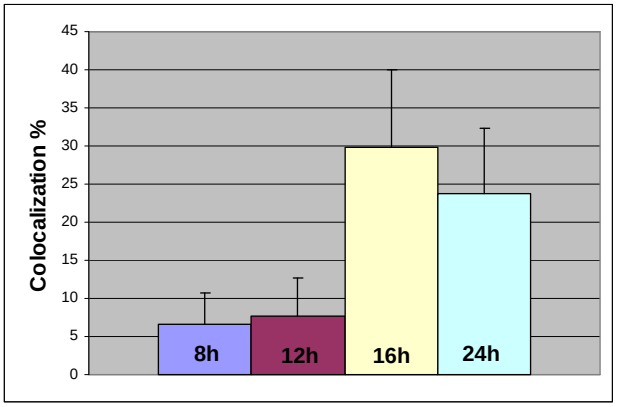

Figure 4.8 Histogram of the average colocalization percents between NS1 and EGFP-PABP2 at four different timepoints (8h, 12h, 16h and 24h) and the variation of the data.

4.1.5 Colocalization between NS1 and EGFP -TFIIB

Examination of the confocal images of NS1 and enhanced green fluorescent protein linked to TFIIB showed rather clear colocalization pattern. Extensive colocalization appeared after the NS1 had spread around nucleus, already at 12h time point. The information of confocal pictures gave a reason to assume that these two proteins colocalize strongly with each other (Fig. 4.9).

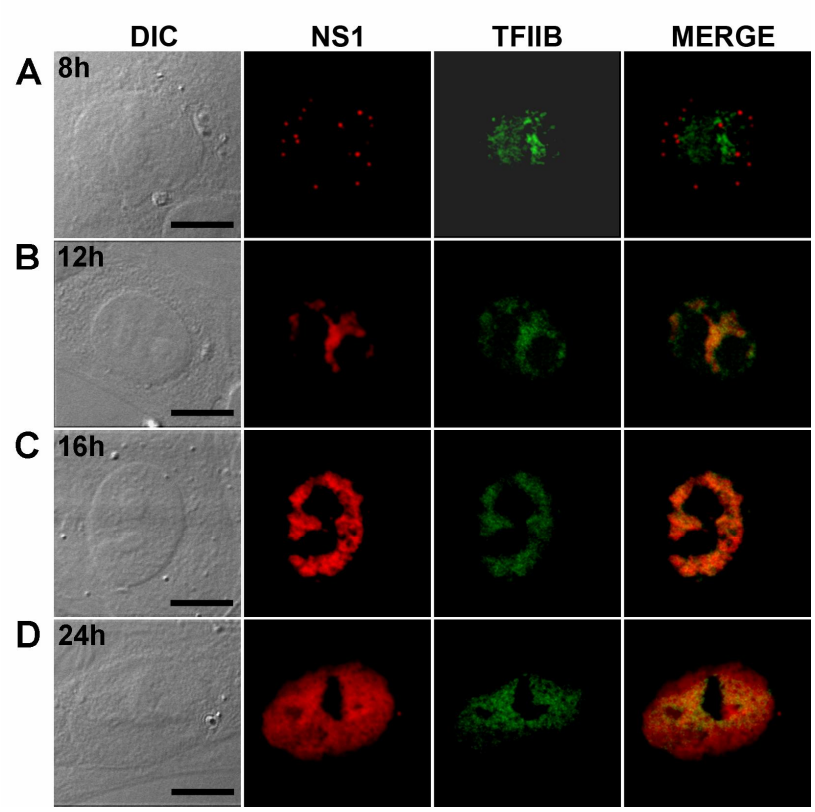

Figure 4.9 Panel of EGFP-TFIIB and NS1 (DIC, NS1, EGFP-TFIIB and merge A) 8h p.i., B) 12h p.i., C) 16h p.i. and D) 24h p.i.. In DIC pictures the scale bare is 5 µm.

The more detail data analysis of the confocal images by ImageJ software confirmed the presumptions that were made according the confocal pictures alone. The colocalization between NS1 and TFIIB was noteworthy after 8h time point (at 8h time point the colocalization was only 1 ± 2 %). The amount of TFIIB colocalizing with NS1 during later phase of infections was 37 ± 31 % at 12h, 45 ± 30 % at 16h and 67 ± 20 % at 24h (Fig. 4.10). The magnitude of colocalization increased strongly along with infection.

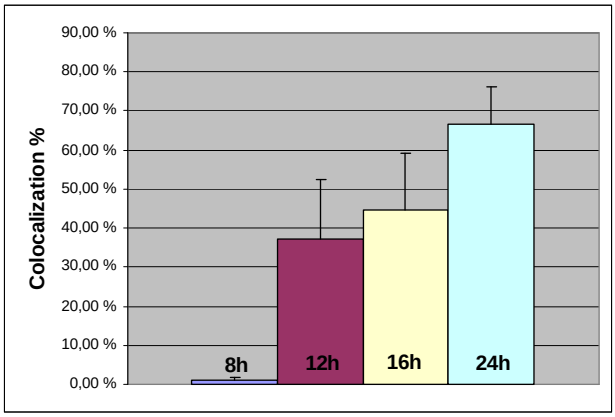

Figure 4.10 Histogram of the average colocalization percents between NS1 and EGFP-TFIIB at four different time points (8h, 12h, 16h and 24h) and the variation of the data.

4.2 Live cell imaging

Since the colocalization studies of NS1 and EGFP-TFIIB suggested that these two proteins localize in same structures with one another, closer examination was conducted. The dynamics of the TFIIB was studied in living cells with the Zeiss confocal microscope. In non-infected cells the TFIIB concentrated inside the nucleolus (Fig. 4.11) whereas during infection the TFIIB situated mostly around the nucleoplasm (Fig. 4.11).

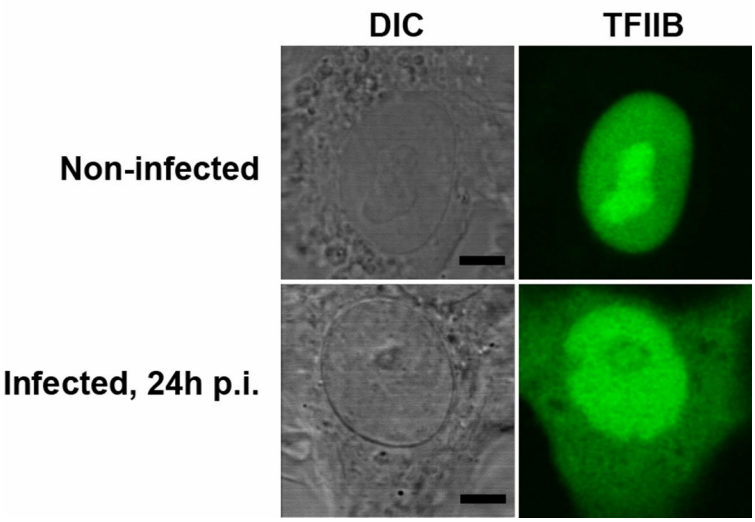

Figure 4.11 Live imaging of EGFP-TFIIB in non-infected and 24h infected cells. In DIC pictures the scale bar is 5 µm.

4.2.1 FRAP

In FRAP (fluorescence recovery after photobleaching) high intensity laser is used to photobleach the fluorescent molecules. By monitoring the fluorescence recovery it is possible to get information about protein mobility and binding properties. In our investigation the possible binding of TFIIB was studied from a certain region of nucleolus, nucleoplasm and infected nucleoplasm (Fig. 4.12 A).

Figure 4.12 A FRAP performed to the nucleoplasm (DIC, nucleus before FRAP, FRAP and nucleus after FRAP). Fluorescence is presented as pseudocolor scale. In the "before the bleach" figure the intensity scale bar is shown.

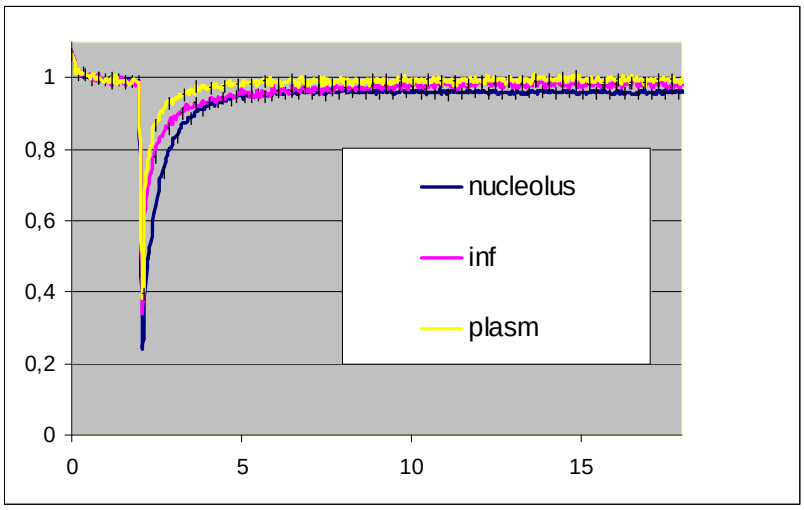

Figure 4.12 B Graphical presentation of the data collected during a FRAP experiment (Blue line demonstrates FRAP performed to non-infected nucleolus, purple line demonstrates FRAP performed to infected nucleoplasm and yellow line demonstrates FRAP performed to non-infected nucleoplasm).

From the graphical presentation of FRAP (Fig. 4.12 B) the assumption can be made that TFIIB has distinct binding states in nucleolus, nucleoplasm and infected nucleoplasm. The fluorescence recovery curve of nucleolus TFIIB (non-infected cell) was slowest and did not return back to the original level. Whereas the fluorescence recovery curve of nucleoplasm (non-infected cell) proved to be fastest indicating that in nucleoplasm the TFIIB is mostly freely diffusing. During the infection the fluorescence signal recovery curve of nucleoplasmic TFIIB lay between the previously mentioned curves.

4.3 Change of nuclear size during infection

Examination of nuclear size during CPV infection was performed with enhanced yellow fluorescent protein fused to H2B histone. The heterochromatin concentrates around the periphery of the nucleus hence the EYFP-H2B reveals the chromosomal territories around the nucleus and can be used to calculate the size of the nucleus.

These studies were also conducted with the Olympus FV-1000 confocal microscope and the data analysis was done by ImageJ software (Abramoff, 2004). 20-30 image stacks were taken per each time point. Examination was performed at 8h, 24h and 48h of post infection (Fig. 4.13).

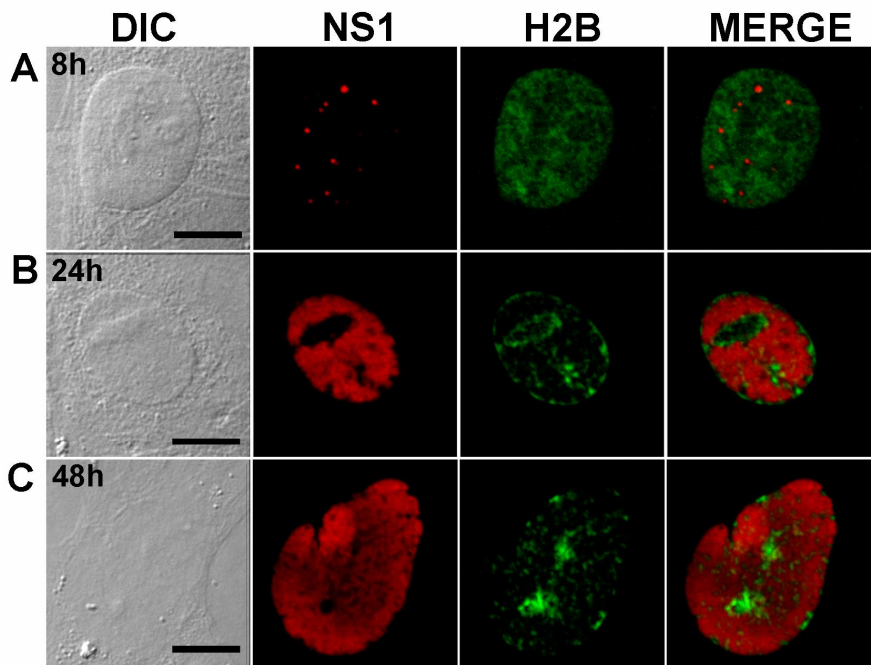

Figure 4.13 Panel of EYFP-H2B and NS1 (DIC, NS1, H2B (chromatin) and merge). A) 8h p.i., B) 24h p.i. and C) 48h p.i.. In DIC pictures the scale bare is 5 μm.

The confocal images gave reason to believe that the size of nucleus grew during the infection (8h-48h). The nucleuses in later phase of infection looked bigger than in the beginning. One more conclusion was made by studying only the merged images. NS1-foci and chromosomal material showed never to colocalize. On the contrary the two proteins were always in distinct regions (Fig. 4.13).

ImageJ software was used to calculate the average nuclear size from the image stacks toward each time point. The results indicated that the size of the nucleus increased during infection 8h-24h (Fig. 14.14). At 48h post infection the chromosomal material was mostly localized in nucleolus (Fig. 4.13 C) H2B). For that reason the ImageJ software was not capable of calculating the size of nucleus at this time point of infection.

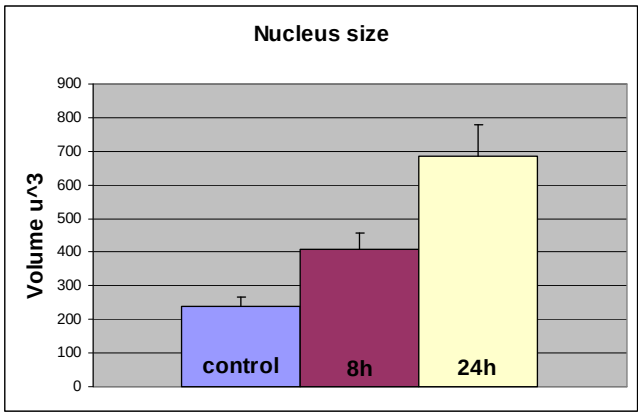

Figure 14.14 Histogram of average nuclear size change during CPV infection. Control/non-infected cells (blue), 8h p.i. (purple) and 24h p.i. (yellow).

The above mentioned software was also used to calculate the average interchromosomal space ("interchromosomal space=volume of nucleus–volume of chromatin"). The interchromosomal space was barely changed when the infection had reached the 8h time point but when the infection proceeded from 8h to 24h the space clearly increased (Fig. 14.15).

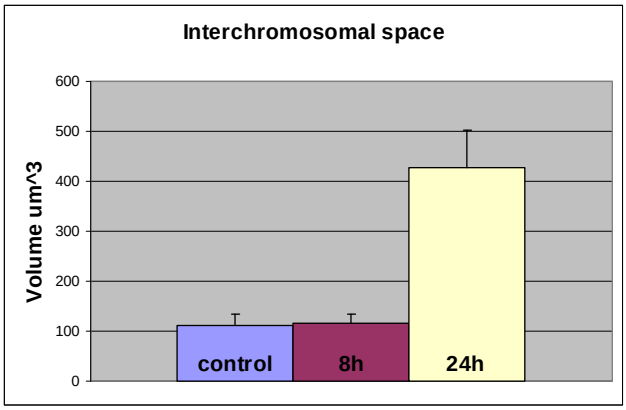

Figure 14.15 Histogram of average interchromosomal volume change during CPV infection. Control/non-infected cells (blue), 8h p.i. (purple) and 24h p.i. (yellow).

5 DISCUSSION

5.1 The colocalization studies

5.1.1 The interaction between PML and NS1

Many viruses have demonstrated to interact with PML NBs during their infection (Everett, R.D., and Maul, G.G., 1994, Ishov, A.M., and Maul, G.G., 1996, Wilkinson, G.W. et al., 1998). According to our study CPV appears to comply with the same kind of behavioral model since the NS1 protein appeared to localize besides the PML NBs in the beginning of the infection.

Compared to any other nuclear proteins (see results of SUMO-1, 2, PABP2 and TFIIB) the colocalization percent was amazingly high already at 8h time point (33 ± 20 %). The analysis of this remarkable colocalization is not unambiguous. The CPV may need PML NBs to modify its own proteins, suggesting that PML NBs are essential for CPV replication. It have already been demonstrated that the MVM requires the CBP (locates in PML NBs) as a transcription factor during the infection (Ohshima, T. et al., 2001). On the other hand the NS1 may interfere with the metabolism of the host cell by affecting some how to the PML NBs thus helping the viral conquest. In this case the PML NBs would work as a part of cell`s intrinsic defence mechanism against CPV infection.

The colocalization after 12h of CPV infection was 19 ± 17 %, lower than the colocalization percent at 8h p.i. The NS1 was no longer found to colocalize with PML NBs as intensively as earlier state of infection. The results suggested that the interaction of these two proteins was not necessary at this state of infection anymore.

Experiments indicated that the colocalization percent was higher at 16h (47 ± 17 %) than at 24h (41 ± 20 %) of post infection. Indeed the confocal pictures demonstrated that PML may localize in space which include no NS1 at later phase of infection. However, when the variation of the data is considered it is hard to indicate whether any noteworthy difference

exists between these two time points. The colocalization percents could simply increase according to the amount of NS1.

5.1.2 The interaction between SUMO-1 and NS1

SUMO-1 has been shown to localize in PML NBs (Zhong, S. et al., 2000a). For this reason it is not surprising that the colocalization pattern of NS1 and SUMO-1 during early phase of infection was similar with NS1 and PML, higher at 8h (20 ± 33 %) than at 12h (8 ± 13 %). The difference is that colocalization percents remained lower between NS1 and SUMO-1 than between NS1 and PML.

At later state the colocalization percents appeared to grow according to the state of the infection. The data illustrated percents being lower at 16h (21 ± 22 %) than at 24h (48 ± 35 %) of post infection. These results differ from the results of PML ($p < 0.05$ %) indicating the possibility that the CPV infection could separate SUMO-1 from PML NBs as some viruses does (Muller, S., and Dejean, A., 1999).

Unfortunately, there were a lot of problems with successful transfections of EYFP-SUMO-1. Thus the colocalization of SUMO-1 and NS1 should be taken into consideration. It was problematic to find the EYFP-SUMO-1 expression and infection from the same nucleus, especially during early phase of infection (8h-12h). If the SUMO-1 expression would have been as rich as the expression of PML the results could have been more similar with these two proteins. For the same reason the variation of the data was greater than with PML.

5.1.3 The interaction between SUMO-2 and NS1

The localization of SUMO-2 has been described quite homogenous inside the nucleus (Ayaydin, F., and Dasso, M., 2004) and this localization pattern is reflected to the results. The present study demonstrates that in the case of EYFP-SUMO-2 and NS1 the colocalization percents clearly stayed low during the whole infection (8h 1 ± 4 %, 12h 6 ± 15 %, 16h 14 ± 18 % and 24h 42 ± 22 %).

Therefore speculation of the results suggests that these two proteins do not interact with each other. On the contrary EYFP-SUMO-2 positive structures and NS1-foci seem to localize randomly. The colocalization increases according to the phase of infection. More the NS1 is expressed the more SUMO-2 colocalize with it. These observations strongly suggest that SUMO-2 is not required for NS1 modification.

5.1.4 The interaction between PABP2 and NS1

The study of EGFP- PABP2 during CPV infection did not show clear colocalization pattern. However, at early state of infection (8h- 12h) the PABP2 and NS1 appeared to locate next to each other. According the confocal images, the distance between these two proteins was nonexistent nevertheless they hardly ever colocalized (8h 7 ± 9 % and 12h 8 ± 10 %). Even in later phase of infection (16h- 24h) when the NS1 had conquered almost the whole nucleus the colocalization percents stayed low (16h 30 ± 21 % and 24h 24 ± 18 %). The percents never passed over 30 %. The PABP2 was found only spaces which include no NS1-foci.

It can be speculated that these proteins are next to each other because they are essential to one another. Past studies have demonstrated PABP2 positioning in speckle structures (Krause, S. et al., 1994), thus the CPV may need the nuclear speckles during the infection. It is also possible that NS1 is somehow linked to PABP2 which would explain why they are situated close to each other. Contrariwise, these two proteins could repel each other. During the later state of infection the PABP2 was continuously found space free of NS1. However, it is possible that at later state of infection the nucleus is crowded of viral material leaving no other opportunity than lie next to each other.

5.1.5 The interaction between TFIIB & NS1

In previous studies, other viruses have already been proved to utilise the TFIIB in transcription activation processes (Jang, H.K. et al., 2001). The confocal pictures of TFIIB and NS1 show a significant fluorescence overlap suggesting that the CPV might use the TFIIB during the infection.

Strong colocalization was observed right after the NS1 started to spread around the nucleus. Already at 12h post infection the colocalization percent was 37 ± 31 %. Based on the data presented, the CPV presumably uses the host cell transcription machinery for its own purposes or at least transcription factors like TFIIB for its activation functions. The findings in the study add TFIIB to a growing list of proteins that probably interact with the NS1 protein of CPV.

This colocalization study of NS1 and different nuclear proteins implies that NS1 protein colocalizes with PML protein and TFIIB protein. Some degree of colocalization was also observed between NS1 and SUMO-1 protein. Any significant colocalization between NS1 and SUMO-2 or PABP2 was not discovered. The aim for the future studies would be to understand the influence of these possible interactions as well as identify other nuclear factors that interact with this interesting viral protein.

The most alarming matter in the colocalization studies would be the fact that there is no guarantee all the cells being in the same time point of infection. The reason for this is that infections will not proceed simultaneous and at same pace in all the cells. This causes variation to the data, especially in later phase of infection. In future studies it could be possible to partly eliminate this variation by studying the colocalization with cell cycle synchronized cells.

The variation of the results can also be caused by different level of protein expression. If the transfection is successful, plenty of proteins are expressed and vice versa. Thus the effectiveness of transfection also affects to the final outcome. The CPV infection should also be equally effective enabling steady expression level of the NS1 protein.

Live cell imaging and FRAP

The previous data described has demonstrated potential physical interactions between NS1 and TFIIB. Live cell imaging revealed more interesting facts about TFIIB. In non-infected cells the TFIIB showed to localize in nucleolus. On the contrary, when the cells were infected the TFIIB located mostly in nucleoplasm. In addition while imaging the fixed cells, TFIIB situated in the nucleoplasm even in non-infected cells. Hence both the infection and the PFA fixing had similar influence on the localization of TFIIB, "releasing" it from the nucleolus to the nucleoplasm.

Live cell imaging indicated that TFIIB changed position between nucleolus and nucleoplasm. As a consequence of CPV infection the TFIIB was shown to localize in nucleoplasm instead of nucleolus. What causes this above mentioned releasing is not known. The liberation of TFIIB to the nucleoplasm after PFA fixing likely occurs because of the strong disturbing effects that PFA have on the nuclear structures.

5.1.6 FRAP (Fluorescence recovery after bleaching)

The FRAP experiments demonstrated that the TFIIB had various recovery dynamics in different locations. The recovery curve of non-infected nucleolus was slowest (Fig. 4.12 B). Inside the nucleolus the only working polymerase is RNA polymerase I hence the binding of TFIIB is not involved in formation of pre-initiation complex (PIC). The nucleolus is however proved to be highly dynamic structure. The nucleolar factors are exchanged with the nucleoplasm (Tsai, R.Y., and McKay, R.D., 2005). Of the many possibilities that could explain the binding; a speculation can be made that TFIIB is temporary stored inside the nucleolus.

The TFIIB recovery curve of nucleoplasm (non-infected cells) returned fast and nicely to the origin level of fluorescence (Fig. 4.12 B). These results indicated that at least part of the TFIIB is freely around nucleoplasm enabling rabid transport of TFIIB to the place where the transcription is about to begin.

When cells were infected, the TFIIB located mostly around nucleoplasm. In FRAP studies of infected cells the recovery curve of nucleoplasm did not return back to the origin level and the recovery was noteworthy slower than in non-infected cells (Fig. 4.12 B). The most reasonable explanation for this is that the transcription has begun and some of the free TFIIB is attached to the already formed pre-initiation complex.

The results of the live cell studies confirmed the previous observations made according the colocalization studies (in fixed cells); TFIIB seem to have a role during CPV infection. In addition interesting facts about TFIIB localization revealed. Further investigations of TFIIB may give more clear identification of the binding, interaction and localization of this protein.

5.2 The size of nucleus during infection

The nuclear size was analysed during CPV infection (0h-48h) by using the yellow fluorescent protein fused to H2B histone. Many DNA viruses replicate in nucleus and previously it has been shown that DNA viruses such as Herpes simplex virus 1, (HSV-1) may cause nuclear expansion and marginalization of host chromatin (Simpson-Holley, M. et al., 2004, Simpson-Holley, M. et al., 2005). The results of this study represent similar kind of outcome than the results of HSV-1. The size of the nucleus grew.

The nuclear size normally complies with the cell cycle. The size increases during S phase (Yang, L. et al., 1997). In this study the non-infected control cells reflects the normal cell grow. However the observed "growth phenomena" during CPV infection showed an abnormal increase. Therefore the replication and multiplied viral material could be one possible explanation for this stunning outcome.

Another possible strategy for the unexpected results might be the lack of small nucleuses in later state of infection. The virus infection causes great stress to the nucleus. The small nucleuses could have been destroyed and vanished as the infection proceeded to the later states. According to this presumption only the biggest nucleuses were alive in later state of infection and no changing of nuclear sizes actually happened.

The results of interchromosomal space calculations ("interchromosomal space=volume of nucleus–volume of chromatin") indicated a growth after 8h of infection. This could be a consequence of the increasing size of nucleus. In addition the CPV can behave like other DNA viruses (like HSV-1) and the increase may also be caused by marginalization of host chromatin. Moreover to total growth of the interchromosomal space could be caused by both above mentioned factors.

In summary this study represented findings how CPV infection effects on nucleus. However further studies are required to perform similar experiments with cell cycle synchronized cells enabling the results to be more accurate. Furthermore in this research the control cells were all fixed at same time point of infection (8h p.i.). To eliminate the potential errors that this might

have caused, every time point should have own control cells.

Overall this study presents entirely new information of the CPV infection. The findings of colocalization and nuclear changes reveal novel details helping us to understand the mysterious life cycle of CPV. However, the significance of the intranuclear interactions requires more examination and the essential reasons regarding the nuclear size changes remain yet to be uncovered.

REFERENCES

Abramoff, M.D., Magelhaes, P.J., Ram, S.J. 2004. "Image Processing with ImageJ". Biophotonics International, volume 11, issue 7, pp. 36-42,

Andrade, L.E., Tan, E.M., and Chan, E.K. 1993. Immunocytochemical analysis of the coiled body in the cell cycle and during cell proliferation. *Proc.Natl.Acad.Sci.U.S.A.* 90:1947-1951.

Ayaydin, F., and Dasso, M. 2004. Distinct in vivo dynamics of vertebrate SUMO paralogues. *Mol.Biol.Cell.* 15:5208-5218.

Barberis, A., Muller, C.W.,Harrison, S.C,Ptashne, M. 1993. Delineation of two functional regions of transcription factor TFIIB. *Proc.Natl.Acad.Sci.U.S.A.* 90:5628-5632.

Barbis, D.P., Chang, S.F., and Parrish, C.R. 1992. Mutations adjacent to the dimple of the canine parvovirus capsid structure affect sialic acid binding. *Virology.* 191:301-308.

Buratowski, S., and Zhou, H. 1993. Functional domains of transcription factor TFIIB. *Proc.Natl.Acad.Sci.U.S.A.* 90:5633-5637.

Bushnell, D.A., Westover, K.D., Davis, R.E., and Kornberg, R.D. 2004. Structural basis of transcription: an RNA polymerase II-TFIIB cocrystal at 4.5 Angstroms. *Science*. 303:983-988.

Calapez, A., Pereira, H.M., Calado, A., Braga, J., Rino, J., Carvalho, C., Tavanez, J.P., Wahle, E., Rosa, A.C., and Carmo-Fonseca, M. 2002. The intranuclear mobility of messenger RNA binding proteins is ATP dependent and temperature sensitive. *J.Cell Biol.* 159:795-805.

Chen, D., Hinkley, C.S., Henry, R.W., and Huang, S. 2002. TBP dynamics in living human cells: constitutive association of TBP with mitotic chromosomes. *Mol.Biol.Cell.* 13:276-284.

Colwill, K., Pawson, T., Andrews, B., Prasad, J., Manley, J.L., Bell, J.C., and Duncan, P.I. 1996. The Clk/Sty protein kinase phosphorylates SR splicing factors and regulates their intranuclear distribution. *EMBO J.* 15:265-275.

Corbau, R., Salom, N., Rommelaere, J., and Nuesch, J.P. 1999. Phosphorylation of the viral nonstructural protein NS1 during MVMp infection of A9 cells. *Virology.* 259:402-415.

Cotmore, S.F., Nuesch, J.P., and Tattersall, P. 1993. Asymmetric resolution of a parvovirus palindrome in vitro. *J.Virol.* 67:1579-1589.

Cotmore, S.F., Nuesch, J.P., and Tattersall, P. 1992. In vitro excision and replication of 5' telomeres of minute virus of mice DNA from cloned palindromic concatemer junctions. *Virology.* 190:365-377.

Cotmore, S.F., and Tattersall, P. 1994. An asymmetric nucleotide in the parvoviral 3' hairpin directs segregation of a single active origin of DNA replication. *EMBO J.* 13:4145-4152.

Cotmore, S.F., and Tattersall, P. 1987. The autonomously replicating parvoviruses of vertebrates. *Adv.Virus Res.* 33:91-174.

Cotmore, S.F., and Tattersall, P. 1986. Organization of nonstructural genes of the autonomous parvovirus minute virus of mice. *J.Virol.* 58:724-732.

Davie, J.R., and Murphy, L.C. 1990. Level of ubiquitinated histone H2B in chromatin is coupled to ongoing transcription. *Biochemistry*. 29:4752-4757.

De la Barre, A.E., Angelov, D., Molla, A., and Dimitrov, S. 2001. The N-terminus of histone H2B, but not that of histone H3 or its phosphorylation, is essential for chromosome condensation. *EMBO J.* 20:6383-6393.

Dellaire, G., and Bazett-Jones, D.P. 2004. PML nuclear bodies: dynamic sensors of DNA damage and cellular stress. *Bioessays.* 26:963-977.

Desterro, J.M., Rodriguez, M.S., Kemp, G.D., and Hay, R.T. 1999. Identification of the enzyme required for activation of the small ubiquitin-like protein SUMO-1. *J.Biol.Chem.* 274:10618-10624.

Dundr, M., Hebert, M.D., Karpova, T.S., Stanek, D., Xu, H., Shpargel, K.B., Meier, U.T., Neugebauer, K.M., Matera, A.G., and Misteli, T. 2004. In vivo kinetics of Cajal body components. *J.Cell Biol.* 164:831-842.

Everett, R.D., and Maul, G.G. 1994. HSV-1 IE protein Vmw110 causes redistribution of PML. *EMBO J.* 13:5062-5069.

Everett, R.D., Meredith, M., Orr, A., Cross, A., Kathoria, M., and Parkinson, J. 1997. A novel ubiquitin-specific protease is dynamically associated with the PML nuclear domain and binds to a herpesvirus regulatory protein. *EMBO J.* 16:566-577.

Everett, R.D., Sourvinos, G., and Orr, A. 2003. Recruitment of herpes simplex virus type 1 transcriptional regulatory protein ICP4 into foci juxtaposed to ND10 in live, infected cells. *J.Virol.* 77:3680-3689.

Freemont, P.S., Hanson, I.M., and Trowsdale, J. 1991. A novel cysteine-rich sequence motif. *Cell.* 64:483-484.

Frugier, T., Nicole, S., Cifuentes-Diaz, C., and Melki, J. 2002. The molecular bases of spinal muscular atrophy. *Curr.Opin.Genet.Dev.* 12:294-298.

Golderer, G., and Grobner, P. 1991. ADP-ribosylation of core histones and their acetylated subspecies. *Biochem.J.* 277 (Pt 3):607-610.

Gostissa, M., Hengstermann, A., Fogal, V., Sandy, P., Schwarz, S.E., Scheffner, M., and Del Sal, G. 1999. Activation of p53 by conjugation to the ubiquitin-like protein SUMO-1. *EMBO J.* 18:6462-6471.

ICTV, International Committee on Taxonomy of Viruses, Seventh Report of the International Committee on Taxonomy, updated on 25 April 2006, access 12.4.07 (http://www.ncbi.nlm.nih.gov/ICTVdb/Ictv/index.htm)

Ing, N.H., Beekman, J.M., Tsai, S.Y., Tsai, M.J., and O'Malley, B.W. 1992. Members of the steroid hormone receptor superfamily interact with TFIIB (S300-II). J.Biol.Chem. 267:17617-17623.

Ishov, A.M., and Maul, G.G. 1996. The periphery of nuclear domain 10 (ND10) as site of DNA virus deposition. *J.Cell Biol.* 134:815-826.

Ito, T., Ikehara, T., Nakagawa, T., Kraus, W.L., and Muramatsu, M. 2000. p300-mediated acetylation facilitates the transfer of histone H2A-H2B dimers from nucleosomes to a histone chaperone. *Genes Dev.* 14:1899-1907.

Jang, H.K., Albrecht, R.A., Buczynski, K.A., Kim, S.K., Derbigny, W.A., and O'Callaghan, D.J. 2001. Mapping the sequences that mediate interaction of the equine herpesvirus 1 immediate-early protein and human TFIIB. *J.Virol.* 75:10219-10230.

Kamitani, T., Kito, K., Nguyen, H.P., Fukuda-Kamitani, T., and Yeh, E.T. 1998. Characterization of a second member of the sentrin family of ubiquitin-like proteins. *J.Biol.Chem.* 273:11349-11353.

Kotaja, N., Karvonen, U., Janne, O.A., and Palvimo, J.J. 2002. PIAS proteins modulate transcription factors by functioning as SUMO-1 ligases. *Mol.Cell.Biol.* 22:5222-5234.

Krause, S., Fakan, S., Weis, K., and Wahle, E. 1994. Immunodetection of poly(A) binding protein II in the cell nucleus. *Exp.Cell Res.* 214:75-82.

Kuhn, U., and Pieler, T. 1996. Xenopus poly(A) binding protein: functional domains in RNA binding and protein-protein interaction. *J.Mol.Biol.* 256:20-30.

Labieniec-Pintel, L., and Pintel, D. 1986. The minute virus of mice P39 transcription unit can encode both capsid proteins. *J.Virol.* 57:1163-1167.

Lamond, A.I., and Sleeman, J.E. 2003. Nuclear substructure and dynamics. *Current Biology.* 13:R825-R828.

LaMorte, V.J., Dyck, J.A., Ochs, R.L., and Evans, R.M. 1998. Localization of nascent RNA and CREB binding protein with the PML-containing nuclear body. *Proc.Natl.Acad.Sci.U.S.A.* 95:4991-4996.

Legendre, D., and Rommelaere, J. 1994. Targeting of promoters for trans activation by a carboxy-terminal domain of the NS-1 protein of the parvovirus minute virus of mice. *J.Virol.* 68:7974-7985.

Legendre, D., and Rommelaere, J. 1992. Terminal regions of the NS-1 protein of the parvovirus minute virus of mice are involved in cytotoxicity and promoter trans inhibition. *J.Virol.* 66:5705-5713.

Liu, Q., and Dreyfuss, G. 1996. A novel nuclear structure containing the survival of motor neurons protein. *EMBO J.* 15:3555-3565.

Malik, S., Lee, D.K., and Roeder, R.G. 1993. Potential RNA polymerase II-induced interactions of transcription factor TFIIB. *Mol.Cell.Biol.* 13:6253-6259.

Matera, A.G. 1999. Nuclear bodies: multifaceted subdomains of the interchromatin space. *Trends Cell Biol.* 9:302-309.

Matunis, M.J., Coutavas, E., and Blobel, G. 1996. A novel ubiquitin-like modification modulates the partitioning of the Ran-GTPase-activating protein RanGAP1 between the cytosol and the nuclear pore complex. *J.Cell Biol.* 135:1457-1470.

Minty, A., Dumont, X., Kaghad, M., and Caput, D. 2000. Covalent modification of p73alpha by SUMO-1. Two-hybrid screening with p73 identifies novel SUMO-1-interacting proteins and a SUMO-1 interaction motif. *J.Biol.Chem.* 275:36316-36323.

Misteli, T., and Spector, D.L. 1997. Protein phosphorylation and the nuclear organization of pre-mRNA splicing. *Trends in Cell Biology.* 7:135-138.

Muller, S., and Dejean, A. 1999. Viral immediate-early proteins abrogate the modification by SUMO-1 of PML and Sp100 proteins, correlating with nuclear body disruption. *J.Virol.* 73:5137-5143.

Muratani, M., Gerlich, D., Janicki, S.M., Gebhard, M., Eils, R., and Spector, D.L. 2002. Metabolic-energy-dependent movement of PML bodies within the mammalian cell nucleus. *Nat.Cell Biol.* 4:106-110.

Nathan, D., Ingvarsdottir, K., Sterner, D.E., Bylebyl, G.R., Dokmanovic, M., Dorsey, J.A., Whelan, K.A., Krsmanovic, M., Lane, W.S., Meluh, P.B., Johnson, E.S., and Berger, S.L. 2006. Histone sumoylation is a negative regulator in Saccharomyces cerevisiae and shows dynamic interplay with positive-acting histone modifications. *Genes Dev.* 20:966-976.

Nemeth, A., Krause, S., Blank, D., Jenny, A., Jeno, P., Lustig, A., and Wahle, E. 1995. Isolation of genomic and cDNA clones encoding bovine poly(A) binding protein II. *Nucleic Acids Res.* 23:4034-4041.

Nuesch, J.P., Dettwiler, S., Corbau, R., and Rommelaere, J. 1998. Replicative functions of minute virus of mice NS1 protein are regulated in vitro by phosphorylation through protein kinase C. *J.Virol.* 72:9966-9977.

Okuma, T., Honda, R., Ichikawa, G., Tsumagari, N., and Yasuda, H. 1999. In vitro SUMO-1 modification requires two enzymatic steps, E1 and E2. *Biochem.Biophys.Res.Commun.* 254:693-698.

Ohshima T., Yoshida E., Nakajima T., Yagami KI and Fukamizu A. 2001. Effects of interaction between parvovirus minute virus of mice NS1 and coactivator CBP on NS1- and p53-transactivation. *Int.J.Mol.Med.* 7:49-54.

Paradiso, P.R., Rhode, S.L.,3rd, and Singer, I.I. 1982. Canine parvovirus: a biochemical and ultrastructural characterization. *J.Gen.Virol.* 62 (Pt 1):113-125.

Parker, J.S., Murphy, W.J., Wang, D., O'Brien, S.J., and Parrish, C.R. 2001. Canine and feline parvoviruses can use human or feline transferrin receptors to bind, enter, and infect cells. *J.Virol.* 75:3896-3902.

Parker, J.S., and Parrish, C.R. 2000. Cellular uptake and infection by canine parvovirus involves rapid dynamin-regulated clathrin-mediated endocytosis, followed by slower intracellular trafficking. *J.Virol.* 74:1919-1930.

Parrish, C.R. 1991. Mapping specific functions in the capsid structure of canine parvovirus and feline panleukopenia virus using infectious plasmid clones. *Virology.* 183:195-205.

Parrish, C.R. 1990. Emergence, natural history, and variation of canine, mink, and feline parvoviruses. *Adv.Virus Res.* 38:403-450.

Pintel, D., Dadachanji, D., Astell, C.R., and Ward, D.C. 1983. The genome of minute virus of mice, an autonomous parvovirus, encodes two overlapping transcription units. *Nucleic Acids Res.* 11:1019-1038.

Rangasamy, D., Woytek, K., Khan, S.A., and Wilson, V.G. 2000. SUMO-1 modification of bovine papillomavirus E1 protein is required for intranuclear accumulation. *J.Biol.Chem.* 275:37999-38004.

Reed, A.P., Jones, E.V., and Miller, T.J. 1988. Nucleotide sequence and genome organization of canine parvovirus. *Journal of Virology.* 62:266-276.

Regad, T., Saib, A., Lallemand-Breitenbach, V., Pandolfi, P.P., de The, H., and Chelbi-Alix, M.K. 2001. PML mediates the interferon-induced antiviral state against a complex retrovirus via its association with the viral transactivator. *EMBO J.* 20:3495-3505.

Rhode, S.L.,3rd, and Richard, S.M. 1987. Characterization of the trans-activation-responsive element of the parvovirus H-1 P38 promoter. *J.Virol.* 61:2807-2815.

Saitoh, H., and Hinchey, J. 2000. Functional heterogeneity of small ubiquitin-related protein modifiers SUMO-1 versus SUMO-2/3. *J.Biol.Chem.* 275:6252-6258.

Schul, W., van Driel, R., and de Jong, L. 1998. A Subset of Poly(A) Polymerase Is Concentrated at Sites of RNA Synthesis and Is Associated with Domains Enriched in Splicing Factors and Poly(A) RNA. *Experimental Cell Research*. 238:1-12.

Schwarz, S.E., Matuschewski, K., Liakopoulos, D., Scheffner, M., and Jentsch, S. 1998. The ubiquitin-like proteins SMT3 and SUMO-1 are conjugated by the UBC9 E2 enzyme. *Proc.Natl.Acad.Sci.U.S.A.* 95:560-564.

Seeler, J.S., Marchio, A., Losson, R., Desterro, J.M., Hay, R.T., Chambon, P., and Dejean, A. 2001. Common properties of nuclear body protein SP100 and TIF1alpha chromatin factor: role of SUMO modification. *Mol.Cell.Biol.* 21:3314-3324.

Simpson-Holley, M., Baines, J., Roller, R., and Knipe, D.M. 2004. Herpes simplex virus 1 U(L)31 and U(L)34 gene products promote the late maturation of viral replication compartments to the nuclear periphery. *J.Virol.* 78:5591-5600.

Simpson-Holley, M., Colgrove, R.C., Nalepa, G., Harper, J.W., and Knipe, D.M. 2005. Identification and functional evaluation of cellular and viral factors involved in the alteration of nuclear architecture during herpes simplex virus 1 infection. *J.Virol.* 79:12840-12851.

Sleeman, J.E., and Lamond, A.I. 1999. Newly assembled snRNPs associate with coiled bodies before speckles, suggesting a nuclear snRNP maturation pathway. *Curr.Biol.* 9:1065-1074.

Spector, D.L., Fu, X.D., and Maniatis, T. 1991. Associations between distinct pre-mRNA splicing components and the cell nucleus. *EMBO J.* 10:3467-3481.

Spector, D.L. 1996. Nuclear Organization and Gene Expression. *Experimental Cell Research*. 229:189-197.

Suikkanen, S., Aaltonen, T., Nevalainen, M., Valilehto, O., Lindholm, L., Vuento, M., and Vihinen-Ranta, M. 2003a. Exploitation of microtubule cytoskeleton and dynein during parvoviral traffic toward the nucleus. *J.Virol.* 77:10270-10279.

Suikkanen, S., Antila, M., Jaatinen, A., Vihinen-Ranta, M., and Vuento, M. 2003b. Release of canine parvovirus from endocytic vesicles. *Virology*. 316:267-280.

Suikkanen, S., Saajarvi, K., Hirsimaki, J., Valilehto, O., Reunanen, H., Vihinen-Ranta, M., and Vuento, M. 2002. Role of recycling endosomes and lysosomes in dynein-dependent entry of canine parvovirus. *J.Virol.* 76:4401-4411.

Trinkle-Mulcahy, L., Sleeman, J.E., and Lamond, A.I. 2001. Dynamic targeting of protein phosphatase 1 within the nuclei of living mammalian cells. *J.Cell.Sci.* 114:4219-4228.

Trowbridge, I.S., and Omary, M.B. 1981. Human cell surface glycoprotein related to cell proliferation is the receptor for transferrin. *Proc.Natl.Acad.Sci.U.S.A.* 78:3039-3043.

Tsai, RY., and McKay, R.D., 2005. A multistep, GTP-driven mechanism controlling the dynamic cycling of nucleostemin. J.Cell Biol. 168:179-184.

Tsao, J., Chapman, M.S., Agbandje, M., Keller, W., Smith, K., Wu, H., Luo, M., Smith, T.J., Rossmann, M.G., and Compans et, a. 1991. The three-dimensional structure of canine parvovirus and its functional implications. Science. 251:1456-1464.

Tullis, G.E., Burger, L.R., and Pintel, D.J. 1992. The trypsin-sensitive RVER domain in the capsid proteins of minute virus of mice is required for efficient cell binding and viral infection but not for proteolytic processing in vivo. *Virology*. 191:846-857.

Vihinen-Ranta, M., Kakkola, L., Kalela, A., Vilja, P., and Vuento, M. 1997. Characterization of a nuclear localization signal of canine parvovirus capsid proteins. *Eur.J.Biochem.* 250:389-394.

Vihinen-Ranta, M., Yuan, W., and Parrish, C.R. 2000. Cytoplasmic trafficking of the canine parvovirus capsid and its role in infection and nuclear transport. *J.Virol.* 74:4853-4859.

Wahle, E. 1995. Poly(A) tail length control is caused by termination of processive synthesis. *J.Biol.Chem.* 270:2800-2808.

Wahle, E., Lustig, A., Jeno, P., and Maurer, P. 1993. Mammalian poly(A)-binding protein II. Physical properties and binding to polynucleotides. *J.Biol.Chem.* 268:2937-2945.

Wahle, E., and Ruegsegger, U. 1999. 3'-End processing of pre-mRNA in eukaryotes. *FEMS Microbiol.Rev.* 23:277-295.

Weidemann, T., Wachsmuth, M., Knoch, T.A., Muller, G., Waldeck, W., and Langowski, J. 2003. Counting Nucleosomes in Living Cells with a Combination of Fluorescence Correlation Spectroscopy and Confocal Imaging. *Journal of Molecular Biology.* 334:229-240.

Wilkinson, G.W., Kelly, C., Sinclair, J.H., and Rickards, C. 1998. Disruption of PML-associated nuclear bodies mediated by the human cytomegalovirus major immediate early gene product. *J.Gen.Virol.* 79 (Pt 5):1233-1245.

Wilson, G.M., Jindal, H.K., Yeung, D.E., Chen, W., and Astell, C.R. 1991. Expression of minute virus of mice major nonstructural protein in insect cells: purification and identification of ATPase and helicase activities. *Virology.* 185:90-98.

Wright, S.J., and Wright, D.J. 2002. Introduction to confocal microscopy. *Methods Cell Biol.* 70:1-85.

Xie, Q., and Chapman, M.S. 1996/12/6. Canine Parvovirus Capsid Structure, Analyzed at 2.9 A Resolution. *Journal of Molecular Biology.* 264:497-520.

Yang, L., Guan, T., and Gerace, L. 1997. Lamin-binding fragment of LAP2 inhibits increase in nuclear volume during the cell cycle and progression into S phase. *J.Cell Biol.* 139:1077-1087.

Zhang, Y., and Xiong, Y. 1999. Mutations in human ARF exon 2 disrupt its nucleolar localization and impair its ability to block nuclear export of MDM2 and p53. *Mol.Cell.* 3:579-591.

Zhong, S., Muller, S., Ronchetti, S., Freemont, P.S., Dejean, A., and Pandolfi, P.P. 2000a. Role of SUMO-1-modified PML in nuclear body formation. *Blood.* 95:2748-2752.

Zhong, S., Salomoni, P., Ronchetti, S., Guo, A., Ruggero, D., and Pandolfi, P.P. 2000b. Promyelocytic leukemia protein (PML) and Daxx participate in a novel nuclear pathway for apoptosis. *J.Exp.Med.* 191:631-640.